sustainability

MDPI

Review

Addressing Hydrogen Sulfide Corrosion in Oil and Gas Industries: A Sustainable Perspective

Mohammadtaghi Vakili *, Petr Koutník and Jan Kohout

ORLEN UniCRE, a.s., Revoluční 1521/84, 400 01 Ústí nad Labem, Czech Republic; petr.koutnik@orlenunicre.cz (P.K.); jan.kohout@orlenunicre.cz (J.K.)
* Correspondence: mohammadtaghi.vakili@orlenunicre.cz

Abstract: In the oil and gas industry, the corrosion attributed to hydrogen sulfide (H_2S) is one of the most significant challenges. This review paper systematically investigates the diverse facets of H_2S corrosion, including its sources, corrosion locations, mechanisms, and resultant corrosion products. Understanding different forms of H_2S corrosion, such as stress-oriented hydrogen-induced cracking (SO-HIC), sulfide stress cracking (SSC), and hydrogen-induced cracking (HIC), provides a thorough comprehension of these phenomena. The paper discusses critical factors influencing H_2S corrosion, such as temperature, flow rate, pH, and H_2S concentration, highlighting their implications for sustainable practices in the oil and gas sector. The review emphasizes the significance of monitoring and mitigation strategies, covering continuous monitoring, applying corrosion inhibitors, selecting materials, and conducting thorough data analysis and reporting. Furthermore, the role of training in fostering a sustainable approach to H_2S corrosion management is highlighted. This exploration advances the overarching goal of sustainable development in the oil and gas industries by providing insights into understanding, monitoring, and mitigating H_2S corrosion. The findings presented here offer a foundation for developing environmentally conscious strategies and practices to guarantee the long-term viability and flexibility of refinery operations.

Keywords: oil and gas industry; hydrogen sulfide corrosion; corrosion mechanisms; corrosion mitigation; sustainable practices

check for updates

Citation: Vakili, M.; Koutník, P.; Kohout, J. Addressing Hydrogen Sulfide Corrosion in Oil and Gas Industries: A Sustainable Perspective. *Sustainability* **2024**, *16*, 1661. https://doi.org/10.3390/su16041661

Academic Editor: Giovanni Esposito

Received: 22 January 2024
Revised: 12 February 2024
Accepted: 16 February 2024
Published: 17 February 2024

Copyright: © 2024 by the authors. Licensee MDPI, Basel, Switzerland. This article is an open access article distributed under the terms and conditions of the Creative Commons Attribution (CC BY) license (https://creativecommons.org/licenses/by/4.0/).

1. Introduction

Pipelines play a crucial role in the oil and gas sector by facilitating the transportation of products to treatment facilities, storage depots, and refinery complexes [1]. Given that these pipelines transport valuable and hazardous substances, any potential failure carries significant financial and environmental consequences, including the risk of catastrophic economic losses and threats to human life [2]. Failures may arise from various factors, including corrosion (external, internal, and stress cracking), mechanical issues (such as material, design, and construction faults), third-party activities (accidental or intentional), operational problems (malfunctions, insufficiencies, disruptions of safeguarding systems, or operator errors), and natural phenomena (such as lightning strikes, floods, or land shifts) [3].

The distribution of failures over 15 years (1990–2005) is illustrated in Figure 1 [4]. Corrosion is the primary contributing factor, accounting for 46.6% of failures in natural gas pipelines and 70.7% in crude oil pipelines. A corrosion cost assessment conducted by a reputable oil and gas corporation revealed that in the fiscal year 2003, expenditures for corrosion amounted to approximately USD 900 million. The global expense attributed to corrosion in the oil and gas sector stands at approximately USD 60 billion. In the United States alone, documented corrosion-related costs in such industries reach USD 1.372 billion. Furthermore, considering the increasing demand for energy sourced from oil and gas and the associated concerns, worldwide corrosion expenses within the industry are expected

to continue to rise [5]. Hence, there is a critical need for proactive risk assessments that balance cost-effectiveness and safety.

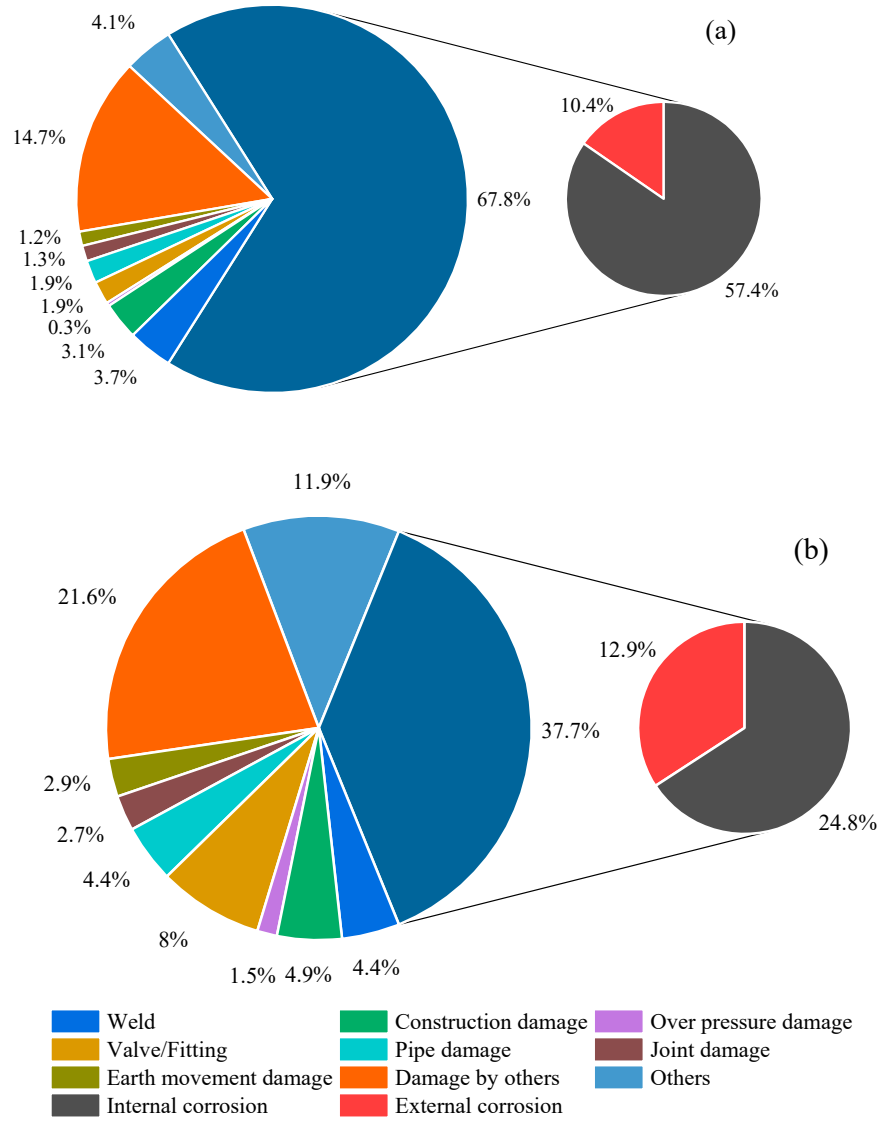

Figure 1. Pipeline incidents by cause (1990–2005): (**a**) crude oil (3826 incidents) and (**b**) natural gas pipelines (411 incidents).

Ensuring the integrity of pipelines is paramount for safe operations, environmental preservation, and the functionality of major production assets. Corrosion poses a serious threat, both externally and internally. External corrosion can result from factors such as oxygen and chloride in the external environment [6]. In contrast, internal corrosion may stem from substances such as hydrogen sulfide (H_2S), carbon dioxide (CO_2), and organic acids present in the production fluid. Unmonitored and uncontrolled pipeline corrosion can lead to leaks and catastrophic failures [7]. Internal corrosion has been a significant concern, constituting approximately 57.4% and 24.8% of corrosion failures in crude oil and natural gas pipelines, respectively (as indicated in Figure 1) [4]. Addressing internal corrosion is imperative for maintaining industry integrity and safety.

In the oil and gas sector, corrosion is typically categorized into two primary types: sweet and sour corrosion, prevalent in environments characterized by elevated partial pressures of H_2S and CO_2 (PH_2S and PCO_2). These particular forms of corrosion represent significant challenges within the industry. Corrosion is further categorized into three regimes

based on the ratio of PCO_2 to PH_2S: sweet corrosion ($PCO_2/PH2S > 500$), sweet–sour corrosion (PCO_2/PH_2S ranging from 20 to 500), and sour corrosion ($PCO_2/PH_2S < 20:1$) [8].

Critical factors influencing corrosion include PH_2S and PCO_2 levels, as well as temperature and pH values. These variables significantly affect the dissolution of corrosive gases, thereby influencing the rate and mechanism of corrosion product formation in sweet and sour environments. Temperature accelerates chemical reactions and increases gas solubility, impacting corrosion rates. pH levels determine environmental acidity or alkalinity, with low pH accelerating corrosion and high pH potentially triggering localized corrosion mechanisms. Dissolved CO_2 and H_2S gases generate corrosive acids in water, reacting with metal surfaces to form less protective compounds, thereby hastening corrosion. Sweet corrosion typically involves the creation of metal carbonates ($MeCO_3$) [9], while sour corrosion involves various metal sulfide formations [10].

In the oil and gas sector, material failures resulting from corrosion in both sour and sweet environments pose various safety, economic, and environmental challenges. Figure 2 shows the relative contribution of various forms of corrosion failures throughout the 1970s [5]. Sour corrosion induced by H_2S is identified as the primary cause of corrosion-related malfunctions in this industry, with its prevalence steadily escalating over time. Proactively addressing sour corrosion and instituting preventive measures are imperative for managing the associated risks in petroleum industries.

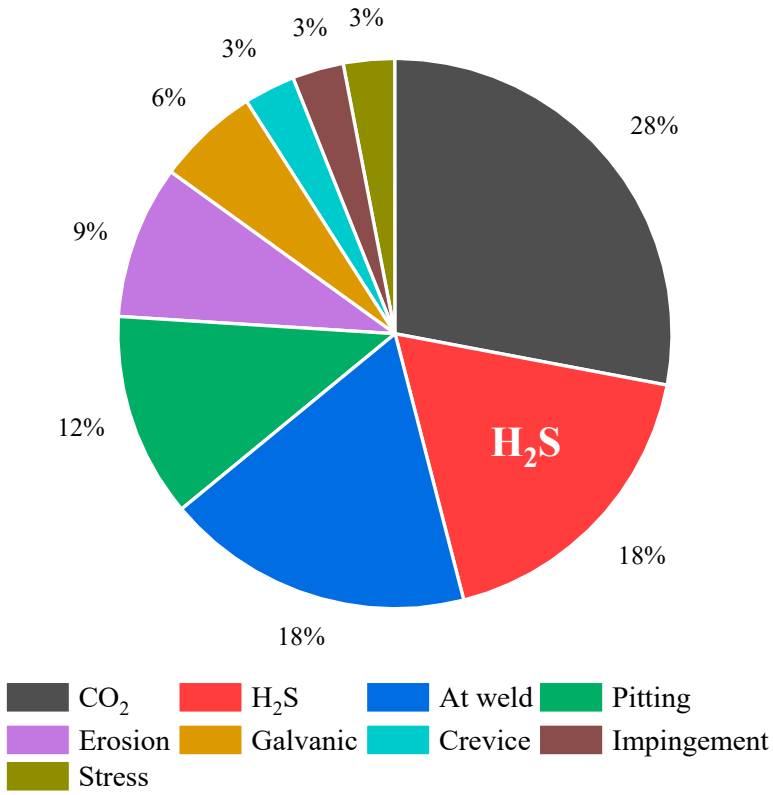

Figure 2. Primary contributors and their respective levels of influence on corrosion-related failures in the oil and gas industry (based on a 1970s study).

Managing and processing substances containing H_2S pose significant challenges in the oil and gas sector. Understanding the intricacies of H2S corrosion is imperative, as it poses a substantial threat to equipment and infrastructure, elevating the risk of structural failure and potential accidents. This type of corrosion evidently diminishes the lifespan of equipment, necessitating costly maintenance or replacement endeavors. Moreover, it impedes operational efficiency, leading to decreased output and heightened energy consumption levels.

Comprehending and addressing the challenges posed by H_2S corrosion within such industries yields noticeable advantages. Safety measures are strengthened by preventing breakdowns and maintaining equipment, and the possibility of accidents and environmental consequences is reduced. This strategy also prolongs the lifespan of equipment, diminishing the need for costly replacements and minimizing the downtime required for repairs. Additionally, it improves operational efficacy by guaranteeing effective and consistent procedures, reducing energy consumption, and reinforcing flow reliability.

Exploring areas for further investigation, including advanced coating technologies, new materials, electrochemical processes, and emerging technologies, is essential. The development of innovative approaches, such as continuous monitoring systems and predictive modeling, shows the potential to enhance precautionary measures. Applying advanced artificial intelligence and advanced analytics in management, prediction, and controlling corrosion is an emerging field that deserves further exploration.

The objective of this study was to compile existing knowledge and explore crucial research areas concerning the prevention of H_2S corrosion in the oil and gas industries. By identifying essential focus areas and potential technological advancements, it aims to provide innovative solutions to uphold the integrity and safety of petroleum and natural gas facilities. This review examines the challenges of H_2S corrosion in such industries and investigates effective mitigation strategies. By investigating the mechanisms, recognizing susceptible equipment and areas prone to H_2S corrosion, and assessing protective measures, the present paper offers valuable insights for researchers and professionals in formulating effective corrosion management strategies. The primary aim is to enhance the understanding of H_2S corrosion in this industry, identify research gaps, and recommend future guidelines for ensuring safe and dependable operation.

2. H_2S Corrosion in Refinery Operations

In refinery operations, H_2S corrosion often arises due to sulfur-containing compounds present in natural gas derived from crude oil, gas wells, and oil well gas. These compounds include thiophenic compounds, sulfur alcohols, elemental sulfur, sulfur ethers, disulfides, and H_2S. Additionally, more complex sulfides, such as metal sulfides, featuring multiple sulfur atoms or intricate molecular structures, may be encountered. These compounds exhibit a wider range of chemical properties and reactivities compared with simpler sulfides, posing potential challenges for corrosion management.

It is important to recognize the role of sulfate-reducing bacteria and microorganisms, which thrive in specific environments and contribute to H_2S production. These bacteria aid in the breakdown of sulfur-containing compounds, releasing H_2S as a byproduct. Moreover, sulfate-reducing bacteria can themselves decompose during formation, leading to H_2S generation. Furthermore, the fluids used in oil and gas wells containing sulfonate can decompose at high temperatures, resulting in H_2S formation. These various sources collectively contribute to the presence of H_2S and the associated risk of corrosion in refinery processes.

2.1. Hydrogen Sulfide (H_2S)

H_2S is a toxic, corrosive, and flammable gas. It is colorless and easily distinguishable by its strong, pungent odor resembling 'rotten eggs or cabbage'. When dissolved in water, H_2S forms hydrosulfuric acid, resulting in a weakly acidic solution. In aqueous media, it readily dissociates into hydrosulfide, but not sulfide [11]. Due to its density being greater than that of air, H_2S tends to accumulate in low-lying areas and depressions. Its ignition temperature is typically recognized as 518 °F (270 °C) [12]. Upon exposure to air, H_2S undergoes rapid oxidation, producing sulfate and sulfur dioxide (SO_2) due to the presence of oxidizing agents such as radicals in the air. This process results in a brief residence time of about 15 days for H_2S in the atmosphere [12]. The lower and upper explosive limits of H_2S are 4% and 44%, respectively. This indicates that H_2S cannot combust in air at

concentrations below 4% or above 44%. Combusting H_2S yields SO_2. Table 1 summarizes the physicochemical properties of H_2S [13].

Table 1. Physical and chemical characteristics of H_2S.

Characteristic	Detail
Chemical structure	
Molar weight	34.08 g mol^{-1}
Odor	Offensive and strong odor of rotten eggs
Color	Colorless
Taste	Sweetish taste
Density	1.5392 g/L
Specific gravity	1.189
Boiling point	−60.25 °C
Melting point	−82 °C
Physical state	Gas
Upper explosive limit (UEL)	44%
Lower explosive limit (LEL)	4%
Auto-ignition temperature	500 °F (260 °C)
Henry's law constant at 25 °C	0.0098 atm-m^3/mol
Vapor pressure at 25 °C	13,600 mmHg
Solubility in water (H_2O)	4 g dm^{-3} (at 20 °C)

2.2. H_2S Sources

In a refinery, H_2S can originate from diverse sources during the processing of crude oil and other hydrocarbon products (Figure 3).

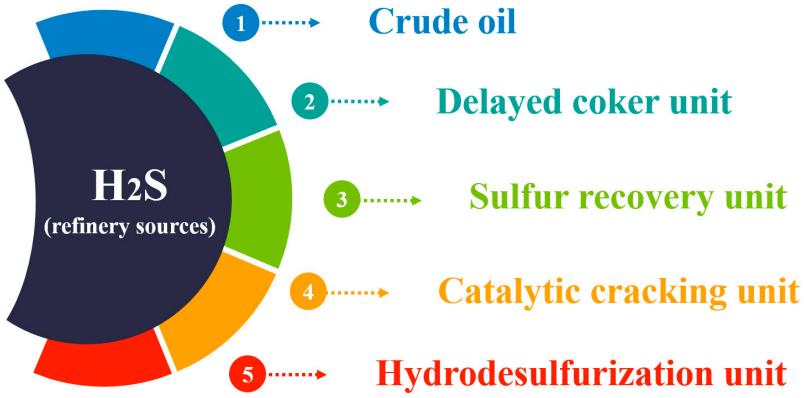

Figure 3. Main H2S sources in the refinery.

- Crude oil serves as the primary source of H_2S within refineries. During processing, naturally occurring sulfur compounds in crude oil release H_2S gas [14]. Crude oil is typically categorized as "sweet" or "sour" based on its sulfur content, with sour crude oil containing higher levels of sulfur compounds, including H_2S.
- Various other sources within refinery facilities can also contribute to H_2S production. Refineries utilize hydrodesulfurization units to efficiently remove sulfur from products such as jet fuel, diesel, and gasoline, converting sulfur compounds into H_2S [15].
- Catalytic reforming is a crucial process in refineries for converting low-octane hydrocarbons into high-octane gasoline blending components. This process can potentially generate H_2S if sulfur-containing compounds are present in the feedstock [16].
- Hydrotreating units utilize hydrogen gas to react with hydrocarbon streams, removing impurities such as sulfur and converting sulfur compounds into H_2S [17].
- Delayed coker units facilitate the conversion of heavy residuals into lighter products, including petroleum coke, which can also release H_2S [18].

- Sulfur recovery units (SRUs) in refineries extract elemental sulfur from sour gases produced during refining processes. H2S is typically converted into elemental sulfur or sulfuric acid in these units. However, incomplete conversion or operational inefficiencies can result in H_2S emissions [19].
- Sulfuric acid alkylation units, during the alkylation process, produce high-octane alkylate using sulfuric acid. While sulfuric acid primarily acts as a catalyst and is not consumed in the reaction, sulfur-containing impurities in the feedstock can lead to the formation of H_2S as a byproduct [20].
- Tank vents and storage facilities, especially those containing sulfur-containing products such as sour crude oil or intermediate products from desulfurization processes, may emit H_2S when vented, particularly during filling or maintenance activities [21].
- Wastewater treatment processes in refineries generate wastewater containing various contaminants, including sulfur compounds. During wastewater treatment, such as biological or chemical processes, H_2S may be produced due to microbial activity or chemical reactions [22].

Figure 3 illustrates the various sources of H_2S in a refinery, including crude oil processing and specific refinery units such as hydrodesulfurization, catalytic cracking, hydrotreating, and delayed coking.

2.3. H_2S Corrosion Locations

Oil and gas reservoirs containing H_2S concentrations exceeding 3 ppm by volume (ppmv) in the gas phase are referred to as sour hydrocarbon systems. The presence of H_2S in these systems can lead to corrosion in downhole tubulars and surface infrastructure, known as sour corrosion. This corrosion is a primary factor in steel equipment failures within the oil and gas industry, particularly when H_2S concentrations are notably higher than those of CO_2 [23]. Sour corrosion presents significant challenges in refineries and other oil and gas facilities. Downhole tubulars are pipes and casings utilized in oil wells, extending from the surface into the wellbore, playing a crucial role in extracting and transporting oil and gas from underground reservoirs. Surface infrastructure encompasses all facilities and equipment above ground, including storage tanks, processing units, and other installations utilized in oil and gas operations. Various sections within a refinery are vulnerable to H_2S corrosion, such as downstream equipment, hydrotreating units, catalytic reforming units, sour water strippers, amine units, flare systems, and heat exchangers (Figure 4).

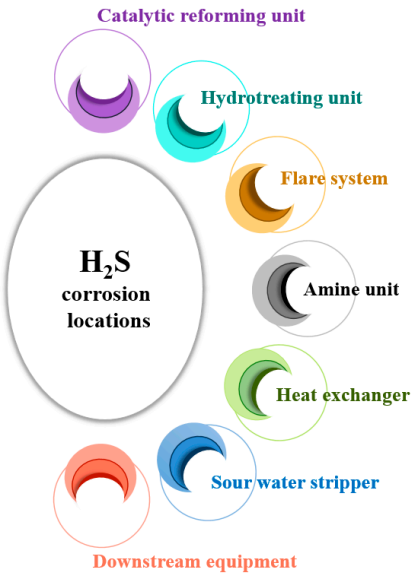

Figure 4. Specific locations susceptible to H_2S corrosion in a refinery.

For example, Liu et al. [24] observed the development of dew point corrosion in the presence of H_2S, leading to the fracturing and perforation of injection pipes. The rupture of the injection tube altered the flow rate and temperature characteristics of the overhead pipe. This corrosion primarily stemmed from the inadequacy of the material chosen for the inhibitor injection tube in this operational environment. Another investigation reported acid gas and sulfur leakage into the air from a refinery's SRU [25]. This leakage happened because of heat exchanger malfunctions in the SRU, which were caused by the corrosion of mild steel equipment. This corrosion was linked to high levels of H2S in the system. The corrosion of steel by H_2S resulted in the formation of iron sulfide, and the subsequent removal of this residue revealed pitting on the steel surface.

2.4. H_2S Corrosion Mechanism

Corrosion in pipelines exposed to sour fluids containing H_2S can arise through several mechanisms. It begins as H_2S gas dissolves in water, leading to the formation of a highly acidic environment. As H_2S dissolves, it promptly undergoes ionization, generating H^+ (hydrogen) and HS^- (bisulfide) ions. Furthermore, HS^- ions may undergo secondary ionization, leading to the release of additional S^{2-} (sulfide) ions and H^+ [26]. The ionization reaction of H_2S is represented by the following equations (Equations (1) and (2)).

$$H_2S \rightleftharpoons H^+ + HS^- \quad (1)$$

$$HS^- \rightleftharpoons H^+ + S^{2-} \quad (2)$$

When H^+ ions make contact with the steel surface, they gain electrons from the metal, undergo a reduction reaction, and subsequently form hydrogen atoms (H_2). This phenomenon is the cathodic reaction. At the same time, the iron (Fe) present in the steel releases an electron, initiating a chemical reaction with S^{2-}, resulting in the formation of iron sulfide (FeS). This reaction is classified as an anodic process [27]. These reactions collectively contribute to the corrosion of steel (Equations (3)–(6)):

$$\text{Anode reaction} : Fe \rightarrow Fe^{2+} + 2e^- \quad (3)$$

$$\text{Anode product} : Fe^{2+} + S^{2-} \rightarrow FeS \quad (4)$$

$$\text{Cathode reaction} : 2H^+ + 2e^- \rightarrow H_2 \quad (5)$$

$$\text{Total reaction} : Fe + H_2S \rightarrow FeS + 2H \quad (6)$$

The reactions have significant consequences:

(a) The formation of a hydrogen atom contributes to hydrogen embrittlement (HE) in steel. When H_2S and/or HS^- are present, the conversion of hydrogen atoms into molecules is hindered, leading to an accumulation of excess hydrogen atoms and increased pressure.

(b) Elevated partial pressure of H_2S leads to decreased pH values in the solution, potentially worsening metal corrosion.

2.5. H_2S Corrosion Products

Hydrogen atoms in steel can result in HE, especially when they are impeded from recombining into hydrogen molecules by H_2S and/or HS^-. Elevated partial pressures of H_2S can exacerbate corrosion by increasing the concentration of the solution and reducing its pH value. In environments with H_2S, high-strength steels such as those used in pipelines and pressure vessels form a natural FeS film on their surfaces. This film acts as a barrier against hydrogen diffusion and promotes hydrogen reduction reactions owing to its favorable electrical conductivity [26]. The type of FeS corrosion product formed depends on factors such as temperature, pH, and H_2S concentration. Examples include troilite, mackinawite, marcasite, pyrrhotite, and kansite [28]. Figure 5 illustrates the relative

percentages of primary corrosion products resulting from the exposure of carbon steel to H_2S-induced corrosion [5].

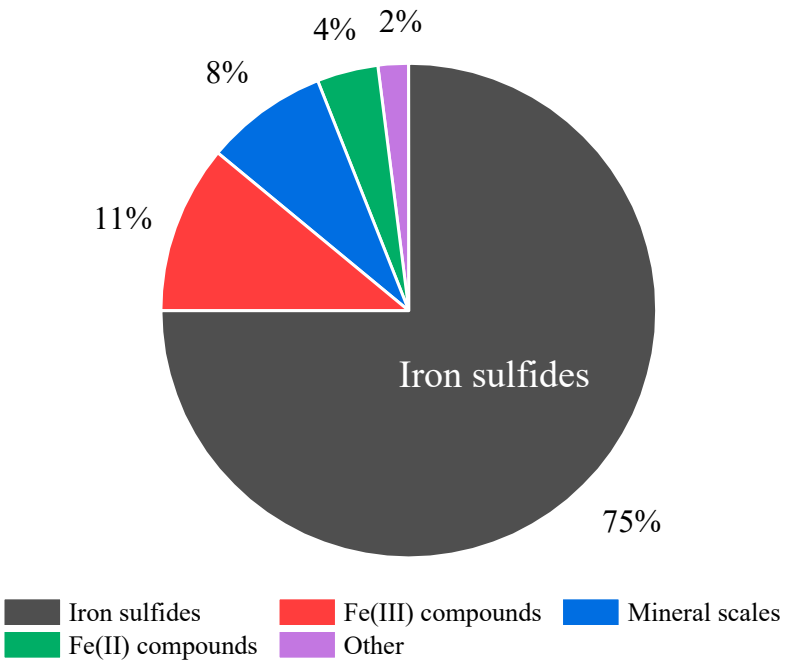

Figure 5. Common H_2S corrosion products and their relative percentage.

Understanding the various forms of FeS corrosion products is essential for developing effective strategies to prevent and mitigate corrosion in environments rich in H_2S. Different forms of FeS demonstrate distinct protective properties and behaviors depending on different conditions. For example, the formation of a protective film by mackinawite results in reduced corrosion rates. However, it is crucial to note that changes in process conditions may reintroduce corrosion risks as fresh mackinawite forms. This comprehension of the behavior of FeS guides engineers and operators in their efforts to maintain the reliability and security of equipment in the petroleum and natural gas industry. Mackinawite is the primary sulfide product in most oil and gas pipelines operating at temperatures below 90 °C. Nevertheless, at higher temperatures, troilite and/or pyrrhotite become the main corrosion products [29].

Mackinawite forms as the initial corrosion product on Fe in H_2S-rich environments, playing a critical role in corrosion processes. Its formation involves complex chemical reactions between Fe and S^{2-}, resulting in a tetragonal crystal structure [30]. The presence of Fe^{2+} ions on its surface make mackinawite highly vulnerable to oxidation when exposed to oxidizing agents. While mackinawite initially reduces corrosion rates, changes in conditions may lead to renewed risks [31].

The chemical bonding properties found within FeS allow for the formation of nonstoichiometric polymorphs, which are distinguished by their high polarizability and layered structures [32]. Mackinawite rapidly becomes the primary product of corrosion on iron immersed in solutions containing H_2S, gradually transforming into pyrrhotite over time. Understanding the characteristics and stability of FeS is facilitated by studying their behavior in oxygen-free H_2S solutions, particularly concerning pH and electrode potential. This knowledge contributes to our understanding of corrosion processes and aids in developing effective strategies to mitigate corrosion [33,34]. Table 2 provides a comprehensive overview of various types of FeS, including their composition, properties, crystal structures, and distribution [5]. Cubic FeS is predominantly found in corrosive environments affecting Fe-based alloys and specific bacterial species. Its structure closely resembles that of sphalerite, with S atoms forming at the vertices of a face-centered cubic lattice and Fe atoms occupying half of the tetrahedral sites. Cubic FeS forms when temperatures drop below 92 °C and

pH levels range from 2 to 6, through the interaction between elemental Fe and sulfur ions in the aqueous phase [35]. Unlike other FeS compounds, cubic FeS is deemed metastable and undergoes phase transitions within a few days at room temperature. Murowchick and Barnes have shown that a pH environment between 4 and 5 and temperatures ranging from 35 to 60 °C facilitate the nucleation of cubic FeS stemming from competing reactions involving Fe^{2+} and S^{2-}. However, the precise mechanism behind cubic FeS formation remains unclear. Within the sphalerite structure, cubic FeS consists of $[Fe_4S_6(H_2O)_4]^{2-}$ groups and the $Fe_4S_6^{2-}$ subunit, which could act as vital precursors in solution. Nonetheless, cubic FeS has not been observed in nature due to its brief existence [35].

Table 2. Characteristics of different iron sulfides.

Name	Formula	Lattice Structure
Amorphous FeS	$Fe(HS)_2$, FeS_x	Nan-crystalline
Mackinawite	$Fe_{1+x}S$, x = 0.005–0.025	Tetragonal
Pyrite	FeS_2	Cubic
Greigite	Fe_3S_4	Cubic
Cubic FeS	FeS	Cubic
Marcasite	FeS_2	Orthorhombic
Pyrrhotite	$Fe_{1-x}S$	Hexagonal
	Fe_7S_8	Monoclinic
Smythite	Fe_9S_{11}, Fe_7S_8	Hexagonal
Troilite	FeS	Hexagonal

Pyrrhotite and troilite are commonly occurring iron–sulfur minerals with distinct structural properties. Pyrrhotite, the most prevalent Fe-S mineral in the solar system, showcases various superstructures rooted in the NiAs crystal configuration. Its formation typically occurs in high-pressure H_2S environments or on metal surfaces with extended service lives. Pyrrhotite tends to manifest as a hexagonal micro-morphology, resulting in a reduced corrosion rate of steel [28,36]. Troilite, a member of the pyrrhotite crystal system, bears similarities to pyrrhotite but boasts a NiAs-type super-structure at room temperature. At specific temperatures, it undergoes phase transitions, namely, α-phase and β-phase transformations, culminating in the conversion to NiAs unit cells. Troilite may also exhibit acicular morphology in H_2S environments [37,38].

Greigite is frequently associated with microbial environments and plays a crucial role in the directional arrangement of magnetic bacteria [39]. Although it is not commonly found in Fe-H_2S-H_2O systems, it may occur in oxygen-containing environments. However, the precise reaction mechanisms governing its formation under such conditions remain elusive. Greigite's anti-spinel structure, akin to ferriferous oxide, comprises two sub-lattices of Fe atoms and a cubic lattice of sulfur ions, which contribute to its unique properties and behavior [35].

In contrast, pyrite, characterized by its cubic crystal structure resembling NaCl, ranks among the most abundant Fe-S minerals in the Earth's crust. Synthesized strawberry pyrite crystal grains have been observed in Fe-H_2S-H_2O systems, particularly in high-sulfur or high-temperature environments. However, their occurrence is not typically noted in low-H_2S environments. Extensive research has been conducted on pyrite formation, highlighting its significance in geological and environmental contexts [35,40].

FeS films present challenges in characterization due to their lack of observable macroscopic crystallinity. Previous studies have indicated that amorphous FeS, potentially in the nanocrystalline mackinawite form, serves as a foundational compound for forming other FeS [41]. The protective properties of the FeS film vary depending on the concentration of H_2S and the pH of the solution [42]. A protective FeS film develops within specific pH ranges, thereby inhibiting metal corrosion. Mackinawite forms under room temperature conditions and nearly neutral pH levels. Amorphous FeS precipitates within the pH range of 5 to 7 [43]. The local pH near the metal surface influences FeS precipitation, while non-conductive films such as ferrous carbonate ($FeCO_3$) act as diffusion barriers against

corrosive species. The quantity of Fe^{2+} significantly impacts the characteristics of the FeS scale, leading to the formation of different types of precipitated films with varied protective properties. The porosity of the film plays a critical role in regulating the corrosion rate under filming conditions, as incomplete films with porosity can create environments conducive to localized metal attack [44].

Researchers have noted that the types of corrosion products formed in systems containing H_2S depend on the prevalence of mackinawite. When H_2S levels are high and Fe^{2+} levels are low, mackinawite typically dominates the scale that develops on steel surfaces. Conversely, when H_2S levels are low and Fe^{2+} levels are high, both $FeCO_3$ and mackinawite can emerge [44]. The presence of H_2S worsens pitting corrosion, resulting in the formation of FeS islands such as mackinawite and possibly smythite within the porous $FeCO_3$ layer [41]. Understanding the transitions between corrosion products, such as the shift from mackinawite to smythite, is crucial for corrosion control. This transition holds significance regarding the potential resurgence of corrosion and its subsequent impact on equipment integrity. As H_2S levels increase, the composition of the corrosion product layer shifts from $FeCO_3$ to mackinawite. Mackinawite films grow rapidly under sufficient H_2S concentration, forming a thin and continuous layer directly on the steel surface due to the chemical interaction between H_2S and steel [41].

The initial formation of a mackinawite film on the steel surface provides protection and significantly reduces the corrosion rate caused by H_2CO_3 [45]. As time passes, the FeS film becomes denser and more crystalline. This transformation occurs as H_2S penetrates the mackinawite layer from the surrounding solution towards the steel surface, which leads to exfoliation. During this exfoliation process, an outer layer with fractures and porosity is formed [45]. Ferrous ions from areas without a mackinawite film migrate and precipitate within the porous film and on its outer surface, resulting in mackinawite formation. Importantly, the overall Fe concentration within the sulfide film often appears to be lower than the Fe depleted due to corrosion, suggesting a migration of FeS or other Fe compounds away from the corroded area. Localized corrosion occurs when the protective sulfide film deteriorates, usually due to mechanical instability or damage, especially in environments with high chloride concentrations. Over time, the mackinawite film may undergo transformations, changing from mackinawite and smythite to different sulfides. This alteration can lead to fracture of the sulfide film and the subsequent exposure of the steel surface, typically at grain boundaries, initiating localized corrosion [46].

When a non-adherent Mackinawite layer becomes electrically bonded to a steel surface, the cathodic process involves hydrogen generation on the Mackinawite. The primary source of acidity in the water phase arises from the dissociation of H_2CO_3. Different forms of FeS result in varying degrees of corrosion when closely associated with a steel surface. Once this corrosion threshold is surpassed, the FeS becomes inactive. Reactivation of dormant sulfides, prompted by changes in process conditions, can lead to renewed corrosion. This reactivation phenomenon is particularly significant for mackinawite and smythite, given their propensity for corrosion upon reactivation. Subjecting dormant sulfides to vacuum and gentle heat can initiate this reactivation process, potentially elevating corrosion rates [46]. The efficacy of the mackinawite layer in providing protection relies on the equilibrium between mackinawite formation and the corrosion rate. Under stable operational conditions, the inclination for corrosion is expected to diminish over time as mackinawite and smythite evolve into pyrrhotite and troilite, owing to the less reversible nature of hydrogen bonding on these sulfides. However, alterations in process conditions may prompt the formation of new mackinawite, leading to renewed corrosion (the resurgence of corrosion on previously dormant sulfides, often triggered by changes in process conditions) [46].

3. H_2S Corrosion Type

Environmental factors significantly contribute to hydrogen-induced embrittlement caused by H_2S, resulting in material fragility. The main types of cracking linked to this

phenomenon include sulfide stress cracking (SSC) and hydrogen-induced cracking (HIC). These cracking modes can arise from various factors, such as the presence of sour gases in pipelines, operational conditions, and material properties. Steel pipelines, commonly used for oil and gas transportation, are especially prone to adverse environmental conditions. These conditions often include microbial-induced corrosion, aggressive anions such as chloride, organic compounds, and acid gases such as H_2S and CO_2. These factors make pipelines vulnerable to corrosion, which generates hydrogen as a byproduct. Essentially, during the corrosion process, steel oxidizes at the anode, producing Fe^{2+} ions that react with H_2S to form FeS precipitates. At the same time, hydrogen ions from H_2S dissociation generate hydrogen gas at the cathodic site. However, the presence of H_2S hinders the formation of hydrogen molecules from H^+ ions, thereby reducing hydrogen production at the steel surface [47].

Some of the atomic hydrogen formed combines to produce hydrogen gas, while the remainder infiltrates the steel's microstructure. However, the presence of a recombination inhibitor such as H_2S hinders the atomic hydrogen recombination process, leading to a significant amount of hydrogen diffusing into the metal [48]. The presence of dissolved hydrogen can adversely affect the steel in several ways:

- Hydrogen atoms tend to recombine at voids and interfaces of inclusions within the steel matrix, forming molecular hydrogen that becomes trapped and is unable to desorb. This can lead to an accumulation of hydrogen partial pressure, potentially resulting in blister formation. Blisters are a common failure mode, particularly observed in low-carbon steel containing elongated inclusions near the steel surface.
- When hydrogen becomes confined within parallel lamination planes, it can initiate small cracks associated with HIC. These microcracks may accumulate and align along residual stresses, facilitating crack propagation. This phenomenon is known as stress-oriented hydrogen-induced cracking (SOHIC).
- Even small amounts of hydrogen, typically measured in parts per million (ppm), can cause embrittlement in high-strength steels under external or residual stress, leading to SSC.

3.1. Hydrogen-Induced Cracking (HIC)

HIC poses a significant threat to pipeline steels used for transporting hydrocarbons contaminated with acids [49]. Also known as HIC or hydrogen blistering, this phenomenon involves recombining diffused atomic hydrogen within the steel, particularly at structural irregularities such as elongated inclusions aligned parallel to the pipeline's surface. Over time, hydrogen molecules accumulate at inclusion interfaces, leading to internal hydrogen partial pressure and the formation of blisters [50]. This intricate process includes hydrogen diffusion into the steel, forming gas pockets, and subsequent pressure buildup, ultimately resulting in pipeline cracks and failure. Various factors significantly influence HIC, including the steel composition, pressure, temperature, and hydrogen concentration [51]. Therefore, implementing appropriate pipeline design, maintenance, and monitoring measures is crucial to mitigate the risk of hydrogen-induced cracking.

HIC is a slow process occurring over several years and is not influenced by external stresses. Failure occurs when blisters or small cracks form in successive layers and interconnect. Steel with low strength and high levels of elongated sulfide inclusions is especially prone to HIC. However, adding microalloying elements can help reduce this vulnerability in steel. Decreasing the sulfide content to less than 0.003 wt% significantly reduces the risk of HIC [52]. The concentration of H_2S in the environment plays a crucial role in controlling HIC, acting as a catalyst for corrosion and hindering the recombination process, speeding up the diffusion of atomic hydrogen within the steel. Steels with a high density of reversible hydrogen traps are more susceptible to HIC due to higher concentrations of mobile hydrogen.

The formation of HIC is a common type of damage expected in environments containing H_2S [53]. This type of cracking occurs internally, without the application of external

loads, facilitated by the absorption of elemental hydrogen and subsequent internal recombination processes. Various microstructural factors influence the material's ability to absorb hydrogen, the diffusion of hydrogen within the material, and its susceptibility to HIC. Understanding the threshold concentration of H_2S that promotes cracking is essential for evaluating structures operating under conditions similar to those of sour environments. Cracking typically occurs near internal discontinuities within the metal when the diffusing hydrogen concentration surpasses the threshold [54]. Carbon steel wires, commonly composed of intermediate- to high-carbon steels containing 0.3 to 0.7 wt% carbon, experience non-uniform plastic strain distribution during the shaping process, resulting in significant residual stresses across the thickness of the wire, impacting its mechanical properties [55,56]. The susceptibility of steel to HIC is closely linked to microstructural characteristics and the interactions of hydrogen atoms with the metallic matrix [54]. Research suggests that the composition of steel and the presence of nonmetallic inclusions contribute to its susceptibility to HIC [57].

In contrast, others attribute HIC susceptibility directly to factors such as microhardness and the type/morphology of microconstituents [58]. Steels with banded pearlitic structures are more prone to cracking than those with a random structure [59,60]. Incorporating this knowledge helps in understanding the broader implications of HIC across various steel applications and underscores the importance of implementing tailored preventive measures and selecting suitable materials.

In summary, hydrogen blistering represents a multifaceted and potentially harmful occurrence within pipelines, characterized by the infiltration of hydrogen atoms into the metal, resulting in the formation of gas-filled cavities. Gaining insight into the mechanisms underlying the initiation and progression of hydrogen blistering is imperative for effective prevention and mitigation strategies, given its propensity to induce structural deterioration and trigger catastrophic failures in pipeline systems.

3.2. Sulfide Stress Cracking (SSC)

SSC has long been identified as a major issue and a primary cause of failures in pipeline steel in environments with high levels of H_2S [61,62]. This problem demands careful attention because it can lead to ruptures in high-pressure gas transmission pipelines. SSC typically occurs unexpectedly during operations, underscoring the necessity for risk-based safety measures in facilities handling corrosive fluids. Hence, ongoing efforts are focused on refining management strategies to tackle this concern effectively [63]. SSC arises from the combined influence of three main factors: the presence of susceptible materials, localized tensile stress exceeding a critical threshold, and exposure to a wet, sour, and corrosive environment.

In environments rich in wet H_2S, hydrogen atoms penetrate the material lattice, facilitated by H_2S catalysis. This penetration occurs through breaches in the protective layer and the formation of small molecular openings on the metal surface. The primary anodic process in the acidic corrosion of steel in the presence of H_2S is the electrochemical dissolution of iron, which releases surface electrons. These electrons are then absorbed by hydrogen atoms, enabling them to combine and form molecular hydrogen. The permeation of molecular hydrogen through the protective film induces pitting corrosion on the steel surface, leading to potential discrepancies and the formation of galvanic cells, initiating the corrosion process. As the surrounding area deepens, cracks form under stress, temporarily halting fracture propagation upon encountering ductile material. However, hydrogen diffusion at the crack tip continues the cycle, resulting in crack propagation through mechanical tearing.

The susceptibility of steel to SSC arises from the diffusion of atomic hydrogen, originating from the cathodic partial reaction during corrosion in an environment containing H_2S [64]. The presence of H_2S hampers the formation of hydrogen molecules. It facilitates their diffusion into the steel lattice, thereby reducing the steel's ability to withstand deformation under either residual or external stress [64]. Various factors, including steel

metallurgy, stress levels, pH, the partial pressure of H_2S, and the presence of chloride ions, play crucial roles in determining steel susceptibility to SSC [65]. In contrast to HIC, which may take years to result in failure, SSC can initiate and propagate to failure within hours. The examination of secondary phases along grain boundaries, known as grain boundary precipitates, has been extensively explored in materials science and engineering [64]. These precipitates significantly alter material properties, encompassing mechanical, electrical, and corrosion resistance attributes. Understanding the mechanisms governing their formation and growth is essential for designing and optimizing materials with desired characteristics. The investigation of grain boundary precipitates presents opportunities for enhancing material properties, particularly in high-temperature applications, and remains an active area of research and development [64].

The process of SSC involves several stages, including hydrogen reduction, adsorption, diffusion, bonding with grain boundary inclusions, and propagation under stress gradients. Heat-affected zones (HAZs) around welds are commonly susceptible to SSC due to the inadequate control of hard phase growth during welding processes [66]. In welding procedures such as single-pass fillet welds, HAZs are particularly prone to SSC, especially in low-strength steel, primarily due to insufficient heat input and improper preheating of the base metal. This vulnerability emphasizes the importance of employing multiphase welding techniques characterized by a higher heat input and appropriate preheating of the base metal. Such methods effectively manage the formation of hard zones in the HAZ, thereby improving weld resistance to SSC [67].

Furthermore, the metallurgical transformations involved in shaping weld joints can significantly influence the microstructure and properties of the metal, particularly within the HAZ. Rapid cooling rates in the weld joint lead to increased lattice defects in both the HAZ and weld zone, intensifying electrochemical activity in these regions. Consequently, the HAZ becomes a sensitive area for SSC, where its likelihood is heightened. The susceptibility of base metal and weld joints to SSC under different potentials highlights the critical role of proper welding techniques in mitigating SSC risks [68].

3.3. Stress-Oriented Hydrogen-Induced Cracking (SOHIC)

SOHIC primarily occurs in low-strength steels with elevated residual stresses, particularly at welds in pipelines, presenting a rare yet significant challenge in industries operating in H_2S environments [69]. It shares similarities with both HIC and SSC, characterized by a stacked array of cracks traversing the material thickness, significantly reducing the load-bearing capacity of components and leading to substantially higher crack growth rates than HIC [70]. Research by Haidemenopoulos et al. [69] on riser steel operating under wet H_2S service conditions revealed that SOHIC cracks initiate from welded zones and propagate along the rolling direction in the middle of the pipe thickness, influenced by severe wet H_2S conditions and complex stress triaxiality. SOHIC represents a unique manifestation of SSC, emerging from pre-existing microcracks induced by hydrogen under tensile stress perpendicular to the direction of the crack. It typically affects carbon in wet, sour environments subjected to applied stress [67]. It often initiates near the weld zone due to residual stresses, even without inclusions and metallurgical defects, and results from hydrogen accumulation, forming minor cracks propagating under applied stress [71]. Table 3 presents a comparative analysis between HIC and SSC [66].

In practice, HAZs adjacent to the weld are susceptible to SSC and SOHIC, and mitigation strategies include preheating the base metal, utilizing low-hydrogen electrodes, applying a low welding current, and considering post-weld heat treatment. Despite being less well understood than HIC and SSC, SOHIC remains a significant concern in sour service environments, necessitating a thorough grasp of factors beyond inherent resistance that influence its occurrence. Due to their high residual stresses from welding and forming processes, spirally welded pipes are particularly prone to SOHIC. Additionally, SOHIC is closely linked with extremely aggressive sour conditions, worsened by the presence of elemental sulfur, which hampers the hydrogen recombination reaction, leading to increased

hydrogen charging into the steel. However, practical guidelines for preventing SOHIC across material, manufacturing, and fabrication domains are currently lacking, emphasizing the ongoing need for research and development efforts to enhance understanding and mitigate the risks associated with SOHIC in H_2S environments [70,72]. To attain a comprehensive understanding, Figure 6 provides an overview of the various forms of internal corrosion resulting from H_2S exposure in pipelines.

Table 3. Comparative analysis of SSC and HIC characteristics.

	SSC	HIC
Material strength	Mainly in high-strength steel	Mainly in low-strength steel
Applied stress	Affects severely	No effect
Crack direction	Perpendicular to stress	Dependent on microstructure
Location	Anywhere	Ingot core
Environment	Can occur even in mildly corrosive media	Highly corrosive conditions, appreciable hydrogen uptake
Microstructure	Critical effect, Q and T treatment enhances SSC resistance	Cleanliness and nonmetallic inclusions are critical

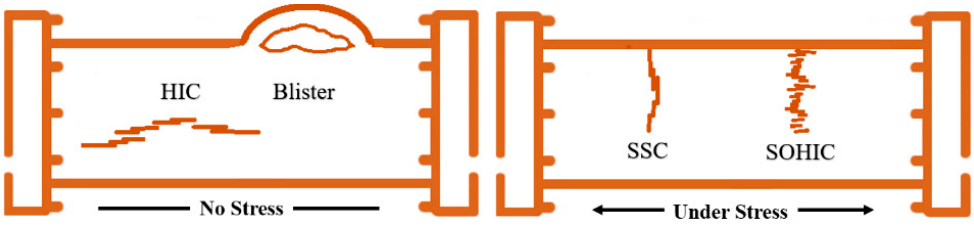

Figure 6. Significant cracking damage caused by H_2S corrosion.

4. Factors Affecting H_2S Corrosion

Several factors play a crucial role in influencing both the occurrence and rate of H_2S corrosion. The formation of a thin, protective layer primarily consisting of FeS, often in the mackinawite form, is vital for preventing corrosion. The development of this passive film is closely linked to the corrosion rate. While other FeS scales such as pyrrhotite, pyrite, and cubic FeS may also be present, they typically exhibit lower adhesion and greater porosity compared with mackinawite. The ability to form and sustain an adhesive scale is influenced by various factors, including temperature, levels of H_2S, impurities in water, properties of the material and electrolyte, flow rates of the fluid, solution pH, and the chemical composition of the steel [29].

4.1. Effect of Temperature

The corrosion resistance of stainless steel decreases at higher temperatures due to forming passive films with more defects. This phenomenon is advantageous in moderating the presence of aggressive ions within the passive film, which speeds up the dissolution process and improves exchange kinetics between the electrode surface and the electrolyte. Elevated temperatures also lead to the creation of a porous film, resulting in a reduction in corrosion resistance [73]. Temperature significantly affects H_2S corrosion in the environment, increasing corrosion rates and reactivity. Higher temperatures cause faster corrosion rates due to the enhanced diffusion of corrosive species and elevated H^+ concentration within the acidic environment (10–25 °C). This increased reactivity intensifies corrosion on metal surfaces, establishing a direct relationship between temperature and the corrosion process. Additionally, higher temperatures exacerbate H_2S corrosion by accelerating chemical reactions, particularly beyond 90–100 °C. The impact of elevated temperatures on H_2S corrosion, including increased corrosion rates and intensified reactivity, is summarized in Figure 7.

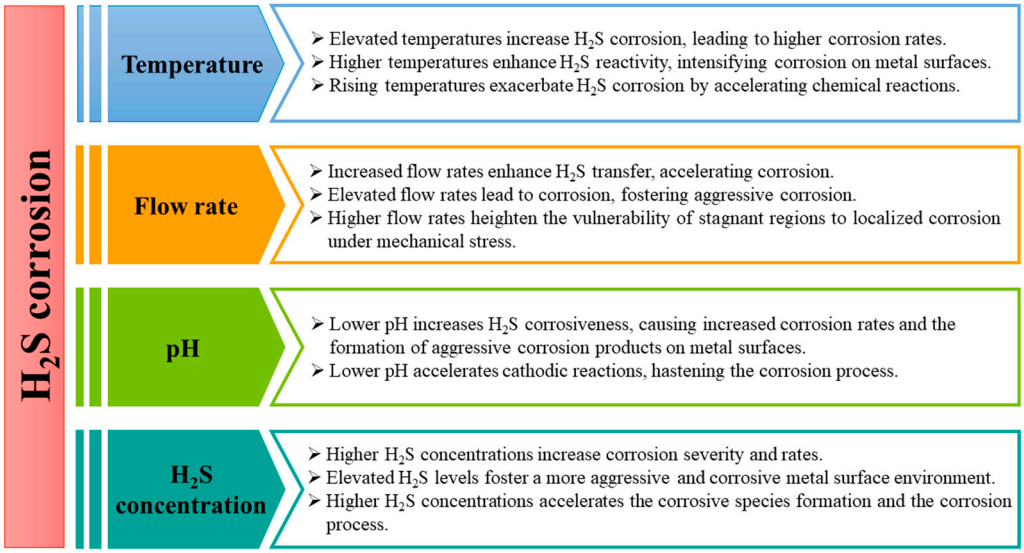

Figure 7. Influence of critical parameters on H_2S corrosion.

Medvedeva et al. [74] found that H_2S in the environment within a temperature range of 20 to 80 °C increases the corrosion rate by 1.5 to 2 times. Zhang et al. [75] noted that the presence of H_2S makes 316 L stainless steel less protective and more sensitive to temperature, while Silva et al. [76] observed severe corrosion of 316 L stainless steel welded plates at temperatures higher than 200 °C. Research on carbon steel by Gao et al. [77] revealed an increase in initial corrosion rates from 2 mm/y to 4 mm/y, eventually stabilizing.

However, the relationship between temperature and corrosion shows a nuanced pattern. At higher temperatures (>100 °C), a decline in corrosion is observed, attributed to higher transport resistance of the corrosion film and reduced H^+ concentration. Mechanisms at elevated temperatures involve reduced gas solubility, leading to increased pH, changes in film formation kinetics, and alterations in corrosion processes at the metal–brine interface. Over time, developing an FeS layer reduces the impact of temperature on the corrosion process, with mackinawite and Fe_3O_4 consistently forming after brief exposure periods. Research suggests that oxide films formed at 250 °C should be more corrosion-resistant and thicker than those at room temperature.

It is important to note that while forming an FeS layer indicates the dominance of "direct" or "solid-state" reactions in influencing the corrosion process, the interplay of elevated temperatures and variations in pH levels can induce thermodynamic modifications. These alterations may ultimately lead to the deterioration of the protective H_2S film, initiating and progressing the formation of pits across the metal surface.

4.2. Effect of Flow Rate

The rate of corrosion on metal surfaces induced by H_2S is significantly influenced by the flow rate, particularly in industries such as oil and gas production. Sun et al. [78] conducted studies revealing that increasing the fluid velocity leads to higher initial corrosion rates, although this effect becomes less pronounced when considering the final corrosion rate. This reduction is likely due to the eventual formation of a protective FeS film. Further investigation emphasizes the significant impact of flow rate on corrosion, attributed to a combination of electrochemical factors and mechanical effects arising from fluid movement. Higher flow rates are closely associated with increased turbulence, which promotes the mixing of solutions and affects the corrosion rate of exposed steel surfaces [79].

Zhang et al. [80] examined the influence of flow rate on the average corrosion rate of L360QS steel, offering additional insights into the effect of flow rate on H_2S corrosion. Corrosion rates remain relatively low at flow rates of 3–6 m/s. However, a significant increase occurs from 0.0132 to 0.1407 mm/a (approximately 10 times) at 6–8 m/s flow rates, respectively. Notably, higher corrosion rates are observed at lower water flow rates due to

inadequate fluid power, resulting in the ineffective removal of sulfur particles and severe corrosion. Conversely, mechanical erosion accelerates the removal of corrosion inhibitors and scales at higher flow speeds, worsening metal corrosion.

Increased turbulence also affects the precipitation rate of $FeCO_3$. Before any film formation, high velocities lead to a higher corrosion rate. Turbulent flow plays a crucial role in facilitating the migration of cathodic species toward the steel surface while simultaneously expediting the transportation of Fe^{2+} ions away from the surface. Consequently, this dual effect reduces the concentration of Fe^{2+} ions at the steel surface, resulting in surface supersaturation. Subsequently, a decrease in the precipitation rate occurs. The implications of flow rate on H_2S corrosion are illustrated in Figure 7.

4.3. Effect of pH

At a given temperature and concentration of H_2S, the rate of corrosion typically decreases as the pH level rises [81]. This decline in corrosion rate occurs because there are fewer H^+ ions available for reduction at cathodic sites. When H_2S is present in trace amounts, the solution becomes under-saturated with $FeCO_3$ and FeS, leading to a gradual reduction in corrosion rate as pH levels increase, particularly noticeable at lower pH values, typically around 4 to 4.5 [82]. However, with an increase in H_2S concentration, the formation of FeS on the metal surface becomes more prominent, exerting significant control over the overall corrosion behavior [83].

The presence of the FeS layer shifts the corrosion mechanism towards the "solid-state" or "direct reduction" reaction of H_2S and Fe, reducing the influence of solution saturation on corrosion. Lower pH levels are associated with an increased corrosiveness of H_2S, resulting in higher corrosion rates and the formation of corrosion-related substances on metal surfaces. This heightened corrosiveness is attributed to the acceleration of cathodic reactions, which accelerates the corrosion process (Figure 7).

It is important to note that a distinct behavior is observed when adjusting pH in a pure H_2S corrosion environment. pH levels also affect the thermodynamic states of FeS. At neutral pH values (around 7), the more thermodynamically stable form of FeS, mackinawite, is formed. However, at lower pH levels (around 4), there is a greater tendency for pyrrhotite formation, which reduces the stability of the FeS film. This shift in the thermodynamic states of FeS due to pH can affect the integrity of the corrosion product layers, potentially leading to pitting corrosion [84,85].

Recent research by Liu et al. [86] further supports the significance of pH in influencing corrosion susceptibility. In low-pH solutions with H_2S, the passive film on the metal is quickly disrupted by H^+ and Cl^- ions generated during cathodic reactions, leading to hydrogen diffusion into the metal and promoting corrosion. As the pH increases, the stability of the passive film improves, inhibiting corrosion. The concentration of H^+ in the solution closely correlates with corrosion susceptibility, with a critical H^+ level above which susceptibility rapidly increases. H_2S acts as both the source of hydrogen for corrosion and a poisoning agent for hydrogen absorption, underscoring the role of H^+ in determining hydrogen generation and concentration on the metal surface. The decrease in pH at the crack tip during crack propagation enhances HE, accelerating corrosion [86].

4.4. Effect of H_2S Concentration

The concentration of H_2S is a critical factor influencing the susceptibility of various steel alloys to corrosion. In environments with consistent pH levels, higher concentrations of H_2S lead to decreased elongation and strength, indicating an increase in susceptibility to corrosion. This effect is primarily due to the corrosive nature of H_2S itself [86]. Moreover, the concentration of H_2S directly affects the corrosion rate of carbon steel, with elevated concentrations correlating with higher levels of corrosion. Tang et al. [87] observed a significant rise in corrosion rates of carbon steel as the concentration of H_2S in the solution increased. For instance, in a solution containing 408.44 mg/L of H_2S, the corrosion rate peaked at 19.06 g m^{-2} h^{-1}, which is nearly 13 times higher than in a solution without

H_2S (approximately 1.50 g m^{-2} h^{-1}). These findings emphasize the substantial impact of increased H_2S concentration on corrosion rates in solutions [87]. This intensified corrosion is attributed to the enhancement of the hydrogen evolution reaction.

Furthermore, the formation of the initial mackinawite film depends on the concentration of H_2S. Predominant corrosion products in environments with low H2S concentrations include mackinawite and cubic FeS [26]. Specifically, the stability of the initial mackinawite film diminishes when H_2S concentrations reach up to 0.035 mol/L, leading to film breakdown and the increased susceptibility of carbon steel to localized corrosion and pitting [88]. Conversely, in environments with high H_2S concentrations, primary corrosion products shift to troilite and pyrrhotite, with some researchers also observing pyrite formation. It is crucial to note that higher concentrations of H_2S intensify both the severity and rate of corrosion, creating a more aggressive and corrosive metal surface environment and accelerating the formation of corrosive species [89]. A visual summary of the significant parameters affecting H_2S corrosion is presented in Figure 7.

5. Monitoring

The effective management of H_2S in refineries is crucial due to its highly corrosive nature. If left unaddressed, it can result in leaks, compromise the structural integrity of equipment, and present significant hazards. Continuous monitoring and the application of corrosion inhibitors are essential for mitigating the potential risks associated with corrosion induced by H_2S. This proactive approach not only extends the lifespan of equipment, but also enhances safety while reducing the financial burden associated with corrosion-related incidents. In refineries, managing the threat of H_2S-induced corrosion requires a well-structured approach. The corrosion monitoring program involves several vital steps: detecting H_2S, monitoring the environment and processes, selecting appropriate materials and conducting corrosion testing, implementing inspection and maintenance protocols, monitoring corrosion inhibitors, and conducting rigorous data analysis and reporting. Furthermore, fostering a culture of training and awareness among personnel strengthens defenses against the risks posed by H_2S corrosion. By implementing this integrated monitoring and preventive strategy, refineries can proactively safeguard their operations against the impact of H_2S-induced corrosion, ensuring reliability, longevity, and adherence to safety standards.

5.1. Continuous Monitoring

Continuous monitoring of H_2S using gas sensors in vital refinery areas is essential for promptly detecting potential risks. The implementation of alarms and automatic shutdown systems for increased H_2S levels enhances safety, ensuring a swift response and minimizing hazards [90]. Furthermore, the deployment of corrosion probes, coupons, or ultrasonic thickness gauges effectively evaluates corrosion rates on metal surfaces exposed to H_2S-containing environments. Regular inspections and analyses of data aid in identifying potential corrosion hotspots. Monitoring process parameters such as pH, flow rates, pressure, and temperature is crucial, as they influence the severity of H_2S corrosion. Tracking process changes or upsets that may elevate H_2S concentration or alter the corrosion environment ensures a comprehensive approach to H_2S corrosion monitoring and mitigation in refinery settings [91]. Regular inspections are vital for detecting early signs of corrosion, such as pitting, scaling, or cracking in equipment exposed to H_2S-containing environments. Timely intervention prevents further deterioration and mitigates potential risks. Additionally, scheduled preventive maintenance and regular cleaning remove accumulated corrosion products, ensuring optimal performance and extending the service life of critical assets. Adherence to these protocols effectively safeguards infrastructure from H_2S-induced corrosion, enhances safety measures, and maintains operational integrity [92].

5.2. Corrosion Coatings

Protective coatings play a crucial role in the oil and gas industries to tackle corrosion challenges, particularly those caused by H_2S in refinery operations. These coatings act as a preventive measure by creating a barrier between metal surfaces and corrosive substances such as H_2S, thereby reducing corrosion rates and improving the longevity and safety of equipment. They offer defense against various degradation mechanisms such as heat, erosion, pitting, and general wear [93,94]. Coatings are typically categorized into three main groups based on the material they are made from: organic, inorganic, and metallic. In refinery environments, all three types are used to protect equipment such as tanks, pipes, and columns from the harmful effects of natural gas, water, and environmental factors. Recent advancements in coating technology have led to the development of specialized formulations tailored to meet the specific demands of the oil and gas industry, thereby optimizing refinery processes [95].

Commonly used coating systems include the three-layer polyolefin (3LPO) and fusion-bonded epoxy (FBE). A high-performance composite coating (HPCC) solution has emerged, offering a single-layer, powder-coated composite system. The HPCC consists of an FBE base coat, a medium-density polyethylene outer coat, and a tie layer containing a chemically modified polyethylene adhesive. Each component is applied using an electrostatic powder coating process, with the tie layer incorporating varying concentrations of FBE. This system provides exceptional adhesion, shear resistance, flexibility at low temperatures, impact and cathodic disbondment resistance to H_2S, and minimal moisture permeability, making it highly effective in protecting various types of steel in crude oil environments [94].

5.3. Cathodic Protection

Cathodic protection (CP) is crucial in combating corrosion in the oil and gas industry, especially in areas where H_2S poses significant risks to buried pipelines and storage facilities [94]. CP works by converting metal surfaces into cathodes within an electrochemical system, aiming to prevent stress corrosion cracking and reduce defects that can occur during the application and operational life of organic coatings, which are the primary methods for managing corrosion [95]. Combining CP with coatings is often seen as the most cost-effective approach for corrosion prevention in refinery environments.

In CP, the goal is to reduce corrosion by minimizing the potential difference between the anode and cathode. This is achieved by applying an external current, such as a pipeline, to the structure being protected. Sufficient current application ensures that the entire structure reaches a uniform potential, eliminating the presence of distinct anode and cathode sites. This method is typically used alongside coatings [96].

Aboveground storage tanks commonly undergo CP on internal and external surfaces in refinery operations. While pure hydrocarbon fluids are generally non-corrosive, internal tank corrosion can occur in areas exposed to sediments, water, and other contaminants [94]. Effective CP operation requires all four fundamental components—anode, cathode, electrolyte, and a complete electrical circuit—to ensure continuous corrosion protection against H_2S. Although corrosion rates of metal structures under CP never reach zero, they are kept exceedingly minimal, reducing the risk of corrosion-induced failures [95].

Two primary CP systems are widely used: sacrificial (or galvanic) anode cathodic protection (SACP) and impressed current cathodic protection (ICCP) [94,96]. SACP involves attaching active metals such as aluminum, zinc, or magnesium to the structure, which sacrificially corrode to protect the metal substrate from the corrosive effects of H_2S [95]. In contrast, ICCP employs an external power source to drive current from inert or low-consumption rate anodes, typically made from graphite, mixed metal oxides, or high-silicon cast Fe [94]. These anodes may be surrounded by carbonaceous backfill to enhance efficiency and reduce costs. Both SACP and ICCP provide effective corrosion protection for various metals and alloys commonly found in refinery infrastructure, including carbon steel, ductile iron, stainless steel, and aluminum [95].

5.4. Corrosion Inhibitor

Corrosion inhibitor monitoring plays a crucial role in protecting metal surfaces from the damaging effects of corrosion induced by H_2S. The organic corrosion inhibitor market has experienced significant growth, accounting for nearly 70% of usage [97]. Inhibitors are administered either through continuous injection or batch treatment, each requiring specific concentration ranges. Continuous injection typically involves concentrations ranging from 10 to 1000 ppm, while batch treatment requires concentrations of 1 to 20 volume percent (% vol). Various types of corrosion inhibitors have demonstrated effectiveness in acidic environments, including polymer-based, Gemini-surfactant-based, water-soluble imidazoline-based, and amine-based inhibitors [10]. Regularly monitoring these inhibitors is essential to ensure they deliver sufficient corrosion protection. This data-driven approach enables industries to adjust inhibitor dosages precisely, ensuring optimal protection and prolonging equipment lifespan. Such a method proves both cost-effective and efficient in combating H_2S-induced corrosion.

5.5. Material Selection

Materials used in acid oil and gas operations still primarily consist of carbon steels. However, there has been a growing trend in using corrosion-resistant alloys (CRAs) for major equipment parts due to advancements in CRAs and the improving economics of these materials. Selecting the right material is crucial to prevent expensive corrosion-related failures and to ensure the safety and reliability of industrial equipment and infrastructure. Materials that resist corrosion from H_2S are particularly important for maintaining the integrity and longevity of equipment and structures in environments containing H_2S. Some materials recognized for their H_2S corrosion resistance include stainless steel, nickel-based alloys, titanium, duplex stainless steels (DSSs), high-density polyethylene, and fiber-reinforced polymers.

Austenitic stainless steels are resistant to corrosion caused by H_2S because of their high Cr content, which leads to the formation of a protective passive layer on the surface [98]. DSS, such as 2205, combines properties of both austenite and ferrite, offering excellent resistance to stress and H_2S corrosion [99]. These steels are highly valued for their strength, toughness, and corrosion resistance, serving as a cost-effective alternative to expensive nickel-based alloys and austenitic stainless steel. The superior corrosion resistance of DSS can be attributed to the formation of a protective passive film and the synergistic effects of their duplex microstructure. In 2205 DSS, this passive film shows heterogeneity, with Mo and Cr concentrated in the ferrite phase and N and Ni in the austenite phase [100]. In environments containing H_2S, the risk of pitting corrosion is increased compared with those with CO_2. Studies by Zheng et al. [101] indicate that pitting corrosion tends to be more severe on the ferrite phase than on the austenite phase in 2205 DSS samples exposed to H_2S-containing environments. Some researchers suggest that the corrosion mechanism of 2205 DSS in H_2S environments differs from that in CO_2 environments due to the role of H_2S in accelerating the dissolution of the passive film and the formation of sulfur corrosion products. Furthermore, it has been observed that 22%Cr DSS can be safely used in environments with high concentrations of H_2S, indicating its suitability for such conditions [100].

Titanium and its alloys exhibit exceptional resistance to corrosion induced by H_2S, especially in acidic environments, thanks to the development of a protective surface layer made of TiO_2 in various corrosive settings [102]. In a study by Thorhallsson and Karlsdottir, 2021 [102], a simulated high-temperature geothermal environment ranging from 180 to 350 °C, with a gauge pressure of 10 bars, was employed. This environment comprised gases such as HCl, H_2S, and CO_2, alongside an acidic condensate with a pH of 3. In this scenario, a specific titanium alloy known as Ti-0.4Ni-3.6Mo-0.75Zr (Ti-475) demonstrated remarkable corrosion resistance, even when exposed to either a single superheated or two-phase condition of the test fluid. This suggests that Ti-475 is a promising choice for casing material in corrosion-prone environments.

Additionally, in a separate research effort, Ti-475 exhibited outstanding resistance to corrosion under simulated high-temperature geothermal conditions. It showed no signs of corrosion even when subjected to either single-superheated or two-phase states of the testing fluid. This exceptional resistance positions Ti-475 as a viable option for applications where corrosion resistance is crucial, particularly in highly corrosive environments. The consistent performance of this alloy under such conditions has established it as a reliable choice for materials requiring high corrosion resistance [103].

Nickel-based alloys are recognized for their outstanding ability to resist corrosion in environments containing H_2S, making them suitable for various applications in the petroleum and natural gas industries. In general, nickel-based alloys exhibit slightly better corrosion resistance than austenitic stainless steels, while austenitic stainless steels demonstrate significantly greater corrosion resistance than ferritic/martensitic steels [104]. The oil and gas sector highly values nickel-based alloys due to their exceptional resistance to corrosion and impressive strength. However, structural changes can occur during solidification, which may lead to solidification cracks and diminished corrosion resistance. Additionally, these alloys may be vulnerable to HE in environments where hydrogen is present, as observed in real-world service conditions [81]. Alloy 625 stands out as a prominent commercial grade among these alloys because of its outstanding corrosion resistance and mechanical properties [105].

Alloy 625, a nickel–chromium alloy solid solution strengthened by Mo and niobium, stands out as a prominent commercial grade. Its corrosion behavior in H_2S environments is influenced by its high alloy content, primarily Ni, Cr, and Mo. While these elements contribute to forming a dense and corrosion-resistant passive film in air, they can also lead to the development of specific microstructures known as Laves and G phases. These phases, which are intermetallic compounds, can have different electrochemical properties compared with the surrounding matrix. As a result, they may be more susceptible to preferential corrosion, meaning they corrode at a different rate or manner compared with the bulk material. In H_2S media, if the passive film breaks down, these distinct phases (Laves and G phases) can accelerate localized corrosion, including pitting corrosion. This is particularly significant when combined with the galvanic mechanism, where there is a significant potential difference between the cathodic (matrix) and anodic (precipitates) regions. Hence, the occurrence of Laves and G phases increases the corrosion tendencies of Inconel 625 in H_2S environments [106].

Steel mills have developed alloys with lower levels of nickel and Mo to provide a stronger alternative to commonly used austenitic stainless steels such as 304L and 316L. Mo enhances the corrosion resistance by increasing the concentration of Mo and Cr in the protective film. This results in a thicker film and a more stable Cr oxide layer. Mo also hinders corrosion through various mechanisms such as adsorption, compound formation, and interaction with other oxides. Additionally, a proposed model suggests that Mo interacts with cation vacancies, limiting their movement and enhancing corrosion resistance [107]. In a study conducted by Tomio et al. [108], various alloys with differing levels of Mo were evaluated for their susceptibility to SCC in the H_2S environment. The results revealed that alloys with lower Mo content (<8%) exhibited higher susceptibility to SCC, as evidenced by a smaller reduction in cross-sectional area and the presence of secondary cracks. Conversely, alloys with higher Mo content (8–16%) exhibited greater resistance to SCC. Microscopic examination of fracture surfaces confirmed Mo's protective role against SCC in this corrosive environment. Furthermore, pitting corrosion was observed in the alloy lacking Mo, indicating a different form of corrosion.

Copper–nickel alloys, known for their high resistance to H_2S corrosion, are widely used in seawater systems. They offer excellent corrosion resistance, machinability, high thermal and electrical conductivity, and moderate resistance to biological scaling [109]. While copper alloys such as brass (a mixture of copper and zinc) find extensive use across various industries, including petrochemicals, they can be susceptible to SCC. This can lead

to cracks, especially under pressure in damp conditions. Brass pipelines are particularly susceptible to corrosion-induced cracking in sulfide-rich environments.

Additionally, brass, especially with high zinc content, is prone to intergranular SCC in the presence of H_2S [110]. For instance, alloys such as $CuZn_{37}$ and $CuZn_{20}Al_2$ are two distinct types of brass alloys suitable for applications in the oil and gas industry. They primarily consist of Cu and Zn, with trace amounts of other elements. $CuZn_{37}$ displays lower resistance to H_2S corrosion, making it less suitable for environments with H_2S content. Conversely, $CuZn_{20}Al_2$ provides enhanced corrosion resistance to H_2S due to the inclusion of aluminum. This makes it a more suitable option for applications in the oil and gas industry, especially in environments with H_2S exposure. However, these alloys' specific use and suitability may also depend on temperature, pressure, and other environmental conditions.

High-density polyethylene is a corrosion-resistant polymer often used in pipeline applications to transport H_2S-containing fluids [111]. Fiber-reinforced polymers, such as fiberglass composites, exhibit good corrosion resistance and are suitable for various applications, including tanks and structural components [112].

5.6. Data Analysis and Reporting

Data analysis and reporting are pivotal in managing corrosion induced by H_2S, enabling industries to glean valuable insights into the corrosion process, pinpoint potential corrosion hotspots, and evaluate the efficacy of corrosion control strategies. By systematically examining data gathered from diverse monitoring systems, industries can make informed decisions regarding the performance of corrosion inhibitors, the state of equipment and structures, and the necessity for maintenance and preventive actions. Furthermore, advanced analytical methods such as predictive modeling and machine learning aid in detecting subtle corrosion patterns, facilitating proactive corrosion control measures. Enhanced data visualization tools also assist in presenting intricate corrosion data in a more user-friendly format, thereby expediting decision-making processes. This analysis aids in recognizing current corrosion trends and forecasting future risks, empowering proactive steps to mitigate substantial damage or downtime due to corrosion-related issues [113,114].

5.7. Training

Training and awareness play crucial roles in managing corrosion induced by H_2S. Effective training programs ensure that personnel working in environments exposed to H_2S understand the corrosion risks and possess the necessary knowledge and skills to implement proper corrosion control measures. By promoting awareness, industries can cultivate a proactive and safety-oriented workforce, thus preventing corrosion-related incidents. Regular training sessions led by experienced professionals help keep the team updated on the latest corrosion mitigation techniques and advanced technologies for early detection. Encouraging active participation in safety protocols and establishing open communication channels for reporting corrosion concerns fosters a culture of vigilance. Conducting periodic emergency response drills ensures preparedness and fosters a collaborative environment that values the contributions of all team members, thus promoting shared responsibility for corrosion control and safety measures [115].

6. Conclusions

In conclusion, effectively addressing H_2S corrosion in the oil and gas industry requires a clearly defined and integrated strategy. Understanding corrosion mechanisms such as HE, HIC, SSC, and SOHIC is crucial for identifying contributing factors and formulating a proactive approach. To ensure equipment longevity, incorporating preventive corrosion monitoring tools such as gas sensors and ultrasonic gauges is essential for early detection and risk mitigation. Material selection is pivotal, mainly focusing on stainless steel, nickel-based alloys, and copper–nickel alloys to combat H_2S-induced corrosion. Careful monitoring and adjustments of corrosion inhibitors are necessary for optimal protection.

Strategic data analysis provides valuable insights into corrosion patterns, supporting informed decision-making processes.

A comprehensive corrosion control strategy involves routine inspections, preventive maintenance measures, and ongoing workforce training. This approach, integrating material science, corrosion engineering, and advanced monitoring technologies, is indispensable for safeguarding assets and minimizing risks associated with H_2S-induced corrosion in the oil and gas sector. Advancements in managing H_2S corrosion are expected. Future perspectives include the integration of advanced technologies, such as real-time monitoring through sensors, to expedite precise corrosion detection. Ongoing research may lead to more resilient alloys and sustainable corrosion inhibitors tailored for H_2S-exposed environments. International collaborations will play a crucial role in fostering global understanding, and continuous workforce training is imperative for staying updated with the latest technologies and best practices. The future outlook involves a dynamic synthesis of technological innovation, material science advancements, and collaborative efforts to ensure the integrity and safety of oil and gas infrastructure amidst evolving challenges.

Author Contributions: M.V., P.K. and J.K. collectively contributed to the conceptualization, literature search, methodology, writing of the original draft, and review and editing of the manuscript. All authors have read and agreed to the published version of the manuscript.

Funding: The publication is a result of the project "Modern trends in the processing of energy raw materials" (8232201) carried out at ORLEN UniCRE a.s.

Institutional Review Board Statement: Not applicable.

Informed Consent Statement: Not applicable.

Data Availability Statement: As a review paper, the information presented in this article is based on the data and findings from the listed source publications in the bibliography.

Conflicts of Interest: The authors declare no conflicts of interest.

References

1. Muthukumar, N. Petroleum products transporting pipeline corrosion—A review. In *The Role of Colloidal Systems in Environmental Protection*; Fanun, M., Ed.; Elsevier: Amsterdam, The Netherlands, 2014; pp. 527–571.
2. Soomro, A.A.; Mokhtar, A.A.; Kurnia, J.C.; Lashari, N.; Lu, H.; Sambo, C. Integrity assessment of corroded oil and gas pipelines using machine learning: A systematic review. *Eng. Fail. Anal.* **2022**, *131*, 105810. [CrossRef]
3. Senouci, A.; Elabbasy, M.; Elwakil, E.; Abdrabou, B.; Zayed, T. A model for predicting failure of oil pipelines. *Struct. Infrastruct. Eng.* **2014**, *10*, 375–387. [CrossRef]
4. Pournara, A.-E. Structural Integrity of Steel Hydrocarbon Pipelines with Local Wall Distortions. Master's Thesis, University of Thessaly, Volos, Greece, 2015.
5. Obot, I.B.; Sorour, A.A.; Verma, C.; Al-Khaldi, T.A.; Rushaid, A.S. Key parameters affecting sweet and sour corrosion: Impact on corrosion risk assessment and inhibition. *Eng. Fail. Anal.* **2023**, *145*, 107008. [CrossRef]
6. Song, C.; Li, Y.; Wu, F.; Luo, J.; Li, L.; Li, G. Failure analysis of the crack and leakage of a crude oil pipeline under CO_2-steam flooding. *Processes* **2023**, *11*, 1567. [CrossRef]
7. Zhao, W.; Zhang, T.; Wang, Y.; Qiao, J.; Wang, Z. Corrosion failure mechanism of associated gas transmission pipeline. *Materials* **2018**, *11*, 1935. [CrossRef]
8. Shi, X.; Zhang, Z.; Wu, L.; Li, X.; Zhang, Z. Corrosion law of metal pipeline in tahe oilfield and application of new materials. *Coatings* **2021**, *11*, 1269. [CrossRef]
9. Videm, K.; Koren, A. Corrosion, passivity, and pitting of carbon steel in aqueous solutions of HCO_3^-, CO_2, and Cl^-. *Corrosion* **1993**, *49*, 746–754. [CrossRef]
10. Obot, I.B.; Solomon, M.M.; Umoren, S.A.; Suleiman, R.; Elanany, M.; Alanazi, N.M.; Sorour, A.A. Progress in the development of sour corrosion inhibitors: Past, present, and future perspectives. *J. Ind. Eng. Chem.* **2019**, *79*, 1–18. [CrossRef]
11. Guidotti, T.L. Hydrogen sulfide intoxication. In *Handbook of Clinical Neurology*; Lotti, M., Bleecker, M.L., Eds.; Elsevier: Amsterdam, The Netherlands, 2015; Volume 131, pp. 111–133.
12. Ausma, T.; De Kok, L.J. Atmospheric H_2S: Impact on plant functioning. *Front. Plant Sci.* **2019**, *10*, 743. [CrossRef]
13. Ahmad, W.; Sethupathi, S.; Kanadasan, G.; Lau, L.C.; Kanthasamy, R. A review on the removal of hydrogen sulfide from biogas by adsorption using sorbents derived from waste. *Rev. Chem. Eng.* **2021**, *37*, 407–431. [CrossRef]
14. Kraia, T.; Varvoutis, G.; Marnellos, G.E.; Konsolakis, M. Unveiling the role of in situ sulfidation and H_2O excess on H_2S decomposition to carbon-free H_2 over cobalt/ceria catalysts. *Catalysts* **2023**, *13*, 504. [CrossRef]

15. Costa, C.; Cornacchia, M.; Pagliero, M.; Fabiano, B.; Vocciante, M.; Reverberi, A.P. Hydrogen sulfide adsorption by iron oxides and their polymer composites: A case-study application to biogas purification. *Materials* **2020**, *13*, 4725. [CrossRef] [PubMed]
16. Afzal, S.; Hussain, H.; Naz, M.Y.; Shukrullah, S.; Ahmad, I.; Irfan, M.; Mursal, S.N.F.; Legutko, S.; Kruszelnicka, I.; Ginter-Kramarczyk, D. Catalytic hydrogen evolution from H_2S cracking over Cr_xZnS Catalyst in a cylindrical single-layered dielectric barrier discharge plasma reactor. *Materials* **2022**, *15*, 7426. [CrossRef] [PubMed]
17. Tian, R.; Xu, W.; Li, Y.; Tian, J.; Wu, L. Energy consumption analysis of a diesel hydrotreating unit using an aspen simulation. *Processes* **2022**, *10*, 2055. [CrossRef]
18. Magomedov, R.; Popova, A.; Maryutina, T.; Kadiev, K.M.; Khadzhiev, S. Current status and prospects of demetallization of heavy petroleum feedstock. *Pet. Chem.* **2015**, *55*, 423–443. [CrossRef]
19. Jagannath, A.; Ibrahim, S.; Raj, A. Heat integration in straight through sulfur recovery units to increase net high pressure steam production. *Chem. Eng. Technol.* **2021**, *44*, 164–173. [CrossRef]
20. Salah, H.B.; Nancarrow, P.; Al-Othman, A. Ionic liquid-assisted refinery processes—A review and industrial perspective. *Fuel* **2021**, *302*, 121195. [CrossRef]
21. Yang, R.; Zhirong, W.; Juncheng, J.; Shuoxun, S.; Peipei, S.; Yawei, L. Cause analysis and prevention measures of fire and explosion caused by sulfur corrosion. *Eng. Fail. Anal.* **2020**, *108*, 104342. [CrossRef]
22. Jiad, M.M.; Abbar, A.H. Petroleum refinery wastewater treatment using a novel combined electro-Fenton and photocatalytic process. *J. Ind. Eng. Chem.* **2024**, *129*, 634–655. [CrossRef]
23. Asadian, M.; Sabzi, M.; Anijdan, S.H.M. The effect of temperature, CO_2, H_2S gases and the resultant iron carbonate and iron sulfide compounds on the sour corrosion behaviour of ASTM A-106 steel for pipeline transportation. *Int. J. Press. Vessels Pip.* **2019**, *171*, 184–193. [CrossRef]
24. Liu, W.; Lyu, Y.; Duan, Z.; Li, W.; Yu, W. Investigation of corrosion sequence in the overhead pipeline of H_2S stripper column through CFD models. *Eng. Fail. Anal.* **2022**, *136*, 106187. [CrossRef]
25. Lins, V.F.C.; Guimarães, E.M. Failure of a heat exchanger generated by an excess of SO_2 and H_2S in the sulfur recovery unit of a petroleum refinery. *J. Loss. Prev. Process. Ind.* **2007**, *20*, 91–97. [CrossRef]
26. Zheng, S.; Zhou, C.; Chen, X.; Zhang, L.; Zheng, J.; Zhao, Y. Dependence of the abnormal protective property on the corrosion product film formed on H_2S-adjacent API-X52 pipeline steel. *Int. J. Hydrogen Energy* **2014**, *39*, 13919–13925. [CrossRef]
27. Lucio-Garcia, M.A.; Gonzalez-Rodriguez, J.G.; Casales, M.; Martinez, L.; Chacon-Nava, J.G.; Neri-Flores, M.A.; Martinez-Villafañe, A. Effect of heat treatment on H_2S corrosion of a micro-alloyed C–Mn steel. *Corros. Sci.* **2009**, *51*, 2380–2386. [CrossRef]
28. Shi, F.; Zhang, L.; Yang, J.; Lu, M.; Ding, J.; Li, H. Polymorphous FeS corrosion products of pipeline steel under highly sour conditions. *Corros. Sci.* **2016**, *102*, 103–113. [CrossRef]
29. Askari, M.; Aliofkhazraei, M.; Afroukhteh, S. A comprehensive review on internal corrosion and cracking of oil and gas pipelines. *J. Nat. Gas Sci. Eng.* **2019**, *71*, 102971. [CrossRef]
30. Ohfuji, H.; Rickard, D. High resolution transmission electron microscopic study of synthetic nanocrystalline mackinawite. *Earth Planet. Sci. Lett.* **2006**, *241*, 227–233. [CrossRef]
31. Boursiquot, S.; Mullet, M.; Abdelmoula, M.; Génin, J.M.; Ehrhardt, J.J. The dry oxidation of tetragonal FeS1-xmackinawite. *Phys. Chem. Miner.* **2001**, *28*, 600–611. [CrossRef]
32. Pearce, C.I.; Pattrick, R.A.; Vaughan, D.J. Electrical and magnetic properties of sulfides. *Rev. Mineral. Geochem.* **2006**, *61*, 127–180. [CrossRef]
33. Davison, W. The solubility of iron sulphides in synthetic and natural waters at ambient temperature. *Aquat. Sci.* **1991**, *53*, 309–329. [CrossRef]
34. Kvarekvål, J.; Moloney, J. 6—Sour corrosion. In *Trends in Oil and Gas Corrosion Research and Technologies*; El-Sherik, A.M., Ed.; Woodhead Publishing: Boston, MA, USA, 2017; pp. 113–147.
35. Wen, X.; Bai, P.; Luo, B.; Zheng, S.; Chen, C. Review of recent progress in the study of corrosion products of steels in a hydrogen sulphide environment. *Corros. Sci.* **2018**, *139*, 124–140. [CrossRef]
36. Ren, C.; Liu, D.; Bai, Z.; Li, T. Corrosion behavior of oil tube steel in simulant solution with hydrogen sulfide and carbon dioxide. *Mater. Chem. Phys.* **2005**, *93*, 305–309. [CrossRef]
37. Skála, R.; Císařová, I.; Drábek, M. Inversion twinning in troilite. *Am. Mineral.* **2006**, *91*, 917–921. [CrossRef]
38. Wang, H.; Salveson, I. A review on the mineral chemistry of the non-stoichiometric iron sulphide, $Fe_{1-x}S$ ($0 \leq x \leq 0.125$): Polymorphs, phase relations and transitions, electronic and magnetic structures. *Phase Transit.* **2005**, *78*, 547–567. [CrossRef]
39. Lefèvre, C.T.; Menguy, N.; Abreu, F.; Lins, U.; Pósfai, M.; Prozorov, T.; Pignol, D.; Frankel, R.B.; Bazylinski, D.A. A cultured greigite-producing magnetotactic bacterium in a novel group of sulfate-reducing bacteria. *Science* **2011**, *334*, 1720–1723. [CrossRef]
40. Kitchaev, D.A.; Ceder, G. Evaluating structure selection in the hydrothermal growth of FeS_2 pyrite and marcasite. *Nat. Commun.* **2016**, *7*, 13799. [CrossRef]
41. Jeong, H.Y.; Lee, J.H.; Hayes, K.F. Characterization of synthetic nanocrystalline mackinawite: Crystal structure, particle size, and specific surface area. *Geochim. Cosmochim. Acta.* **2008**, *72*, 493–505. [CrossRef] [PubMed]
42. Ma, H.; Cheng, X.; Chen, S.; Li, G.; Chen, X.; Lei, S.; Yang, H. Theoretical interpretation on impedance spectra for anodic iron dissolution in acidic solutions containing hydrogen sulfide. *Corrosion* **1998**, *54*, 634–640. [CrossRef]
43. Ma, H.; Cheng, X.; Li, G.; Chen, S.; Quan, Z.; Zhao, S.; Niu, L. The influence of hydrogen sulfide on corrosion of iron under different conditions. *Corros. Sci.* **2000**, *42*, 1669–1683. [CrossRef]

44. Sun, W.; Nesic, S.; Papavinasam, S. Kinetics of iron sulfide and mixed iron sulfide/carbonate scale precipitation in CO_2/H_2S corrosion. In *Nace Corrosion*; NACE: Bethlehem, PA, USA, 2006; p. NACE-06644.
45. Zheng, Y.; Ning, J.; Brown, B.; Young, D.; Nesic, S. Mechanistic study of the effect of iron sulfide layers on hydrogen sulfide corrosion of carbon steel. In *Nace Corrosion*; NACE: Bethlehem, PA, USA, 2015; p. NACE-2015-5933.
46. King, R.A. 11—Sulfide stress cracking. In *Trends in Oil and Gas Corrosion Research and Technologies*; El-Sherik, A.M., Ed.; Woodhead Publishing: Boston, MA, USA, 2017; pp. 271–294.
47. Rickard, D.; Luther, G.W. Chemistry of iron sulfides. *Chem. Rev.* **2007**, *107*, 514–562. [CrossRef] [PubMed]
48. Ossai, C.I.; Boswell, B.; Davies, I.J. Pipeline failures in corrosive environments—A conceptual analysis of trends and effects. *Eng. Fail. Anal.* **2015**, *53*, 36–58. [CrossRef]
49. Anijdan, S.M.; Arab, G.; Sabzi, M.; Sadeghi, M.; Eivani, A.R.; Jafarian, H.R. Sensitivity to hydrogen induced cracking, and corrosion performance of an API X65 pipeline steel in H_2S containing environment: Influence of heat treatment and its subsequent microstructural changes. *J. Mater. Res. Technol.* **2021**, *15*, 1–16. [CrossRef]
50. Abdelshafeek, K.A.; Abdallah, W.E.; Elsayed, W.M.; Eladawy, H.A.; El-Shamy, A. Vicia faba peel extracts bearing fatty acids moieties as a cost-effective and green corrosion inhibitor for mild steel in marine water: Computational and electrochemical studies. *Sci. Rep.* **2022**, *12*, 20611. [CrossRef] [PubMed]
51. Bertoncello, J.C.B.; Simoni, L.; Tagliari, M.R.; Scheid, A.; Paes, M.T.P.; Kwietniewski, C.E.F. Effects of thermal spray aluminium coating on SSC and HIC resistance of high strength steel in a sour environment. *Surf. Coat. Technol.* **2020**, *399*, 126156. [CrossRef]
52. Traidia, A.; Alfano, M.; Lubineau, G.; Duval, S.; Sherik, A. An effective finite element model for the prediction of hydrogen induced cracking in steel pipelines. *Int. J. Hydrogen Energy* **2012**, *37*, 16214–16230. [CrossRef]
53. Martin, M.L.; Sofronis, P. Hydrogen-induced cracking and blistering in steels: A review. *J. Nat. Gas Eng.* **2022**, *101*, 104547. [CrossRef]
54. Campos, E.S.; de Sá, J.D.S.; Campos, T.S.; de Souza, E.A.; Gomes, J.A.D.C.P. Influence of metallurgical factors on the hydrogen induced cracking of carbon steel wires in H_2S-containing environments. *Eng. Fail. Anal.* **2024**, *155*, 107739. [CrossRef]
55. Toribio, J.; Lorenzo, M.; Vergara, D.; Aguado, L. Residual stress redistribution induced by fatigue in cold-drawn prestressing steel wires. *Constr. Build. Mater.* **2016**, *114*, 317–322. [CrossRef]
56. De Giorgi, M. Residual stress evolution in cold-rolled steels. *Int. J. Fatigue* **2011**, *33*, 507–512. [CrossRef]
57. Domizzi, G.; Anteri, G.; Ovejero-García, J. Influence of sulphur content and inclusion distribution on the hydrogen induced blister cracking in pressure vessel and pipeline steels. *Corros. Sci.* **2001**, *43*, 325–339. [CrossRef]
58. Mohtadi-Bonab, M.A.; Szpunar, J.A.; Razavi-Tousi, S.S. A comparative study of hydrogen induced cracking behavior in API 5L X60 and X70 pipeline steels. *Eng. Fail. Anal.* **2013**, *33*, 163–175. [CrossRef]
59. Lee, H.-L.; Lap-Ip Chan, S. Hydrogen embrittlement of AISI 4130 steel with an alternate ferrite/pearlite banded structure. *Mater. Sci. Eng. A* **1991**, *142*, 193–201. [CrossRef]
60. Tau, L.; Chan, S.L.I. Effects of ferrite/pearlite alignment on the hydrogen permeation in a AISI 4130 steel. *Mater. Lett.* **1996**, *29*, 143–147. [CrossRef]
61. Roccisano, A.; Nafisi, S.; Ghomashchi, R. Stress corrosion cracking observed in ex-service gas pipelines: A comprehensive study. *Metall. Mater. Trans. A* **2020**, *51*, 167–188. [CrossRef]
62. Wang, Q.; Sun, Y.; Shi, G.; Meng, K.; Wang, Q.; Zhang, F. Effect of niobium on sulfide stress cracking behavior of tempered martensitic steel. *Corros. Sci.* **2020**, *165*, 108387. [CrossRef]
63. Zvirko, O.; Gabetta, G.; Tsyrulnyk, O.; Kret, N. Assessment of in-service degradation of gas pipeline steel taking into account susceptibility to stress corrosion cracking. *Procedia Struct. Integr.* **2019**, *16*, 121–125. [CrossRef]
64. Sherif, E.-S.M.; Abbas, A.T.; Gopi, D.; El-Shamy, A. Corrosion and corrosion inhibition of high strength low alloy steel in 2.0 M sulfuric acid solutions by 3-amino-1,2,3-triazole as a corrosion inhibitor. *J. Chem.* **2014**, *2014*, 538794. [CrossRef]
65. Sherif, E.-S.M.; Abbas, A.T.; Halfa, H.; El-Shamy, A.M. Corrosion of high strength steel in concentrated sulfuric acid pickling solutions and its inhibition by 3-amino-5-mercapto-1,2,3-triazole. *Int. J. Electrochem. Sci.* **2015**, *10*, 1777–1791. [CrossRef]
66. Chong, T.-V.S.; Kumar, S.B.; Lai, M.O.; Loh, W.L. Effects of wet H_2S containing environment on mechanical properties of NACE grade C–Mn steel pipeline girth welds. *Eng. Fract. Mech.* **2014**, *131*, 485–503. [CrossRef]
67. El-Shamy, A.M.; Abdelfattah, I.; Elshafey, O.I.; Shehata, M.F. Potential removal of organic loads from petroleum wastewater and its effect on the corrosion behavior of municipal networks. *J. Environ. Manag.* **2018**, *219*, 325–331. [CrossRef]
68. Suman, S.; Biswas, P. Comparative study on SAW welding induced distortion and residual stresses of CSEF steel considering solid state phase transformation and preheating. *J. Manuf. Process.* **2020**, *51*, 19–30. [CrossRef]
69. Haidemenopoulos, G.N.; Kamoutsi, H.; Polychronopoulou, K.; Papageorgiou, P.; Altanis, I.; Dimitriadis, P.; Stiakakis, M. Investigation of stress-oriented hydrogen-induced cracking (SOHIC) in an amine absorber column of an oil refinery. *Metals* **2018**, *8*, 663. [CrossRef]
70. Al-Anezi, M.A.; Rao, S. Failures by SOHIC in sour hydrocarbon service. *J. Fail. Anal. Prev.* **2011**, *11*, 363–371. [CrossRef]
71. El-Shamy, A.M. Fabrication of commercial nanoporous alumina by low voltage anodizing. *Egypt. J. Chem.* **2018**, *61*, 175–185. [CrossRef]
72. Mohtadi-Bonab, M.A.; Mousavi, H.; Pourazizi, R.; Szpunar, J.A. Finite element modeling of HIC propagation in pipeline steel with regard to experimental observations. *Int. J. Hydrogen Energy* **2020**, *45*, 23122–23133. [CrossRef]

73. Wang, Z.; Feng, Z.; Zhang, L. Effect of high temperature on the corrosion behavior and passive film composition of 316 L stainless steel in high H_2S-containing environments. *Corros. Sci.* **2020**, *174*, 108844. [CrossRef]
74. Medvedeva, M. Specifics of high-temperature corrosion processes during oil recovery. *Chem. Pet. Eng.* **2000**, *36*, 749–754. [CrossRef]
75. Zhang, L.; Tang, X.; Wang, Z.; Li, T.; Zhang, Z.; Lu, M. The corrosion behavior of 316L stainless steel in H_2S environment at high temperatures. *Int. J. Electrochem. Sci.* **2017**, *12*, 8806–8819. [CrossRef]
76. Silva, C.C.; Farias, J.P.; de Sant'Ana, H.B. Evaluation of AISI 316L stainless steel welded plates in heavy petroleum environment. *Mater. Des.* **2009**, *30*, 1581–1587. [CrossRef]
77. Gao, S.; Jin, P.; Brown, B.; Young, D.; Nešić, S.; Singer, M. Effect of high temperature on the aqueous H_2S corrosion of mild steel. *Corrosion* **2017**, *73*, 1188–1191. [CrossRef] [PubMed]
78. Sun, W.; Nešic, S.; Papavinasam, S. Kinetics of corrosion layer formation. Part 2—Iron sulfide and mixed iron sulfide/carbonate layers in carbon dioxide/hydrogen sulfide corrosion. *Corrosion* **2008**, *64*, 586–599. [CrossRef]
79. Asmara, Y.P. The roles of H_2S gas in behavior of carbon steel corrosion in oil and gas environment: A review. *J. Tek. Mesin* **2018**, *7*, 37–43. [CrossRef]
80. Zhang, N.; Zeng, D.; Zhang, Z.; Zhao, W.; Yao, G. Effect of flow velocity on pipeline steel corrosion behaviour in H_2S/CO_2 environment with sulphur deposition. *Corros. Eng. Sci. Technol.* **2018**, *53*, 370–377. [CrossRef]
81. Martelo, D.; Sampath, D.; Monici, A.; Morana, R.; Akid, R. Correlative analysis of digital imaging, acoustic emission, and fracture surface topography on hydrogen assisted cracking in Ni-alloy 625+. *Eng. Fract. Mech.* **2019**, *221*, 106678. [CrossRef]
82. Farhadian, A.; Go, W.; Yun, S.; Rahimi, A.; Reza Nabid, M.; Iravani, D.; Seo, Y. Efficient dual-function inhibitors for prevention of gas hydrate formation and CO_2/H_2S corrosion inside oil and gas pipelines. *J. Chem. Eng.* **2022**, *431*, 134098. [CrossRef]
83. Kermani, M.; Morshed, A. Carbon dioxide corrosion in oil and gas productiona compendium. *Corrosion* **2003**, *59*, 659–683. [CrossRef]
84. Nešic, S.; Li, H.; Huang, J.; Sormaz, D. An open source mechanistic model for CO_2/H_2S corrosion of carbon steel. In *Nace Corrosion*; NACE: Bethlehem, PA, USA, 2009; p. NACE-09572.
85. Brown, B.; Nešic, S. Aspects of localized corrosion in an H_2S/CO_2 environment. In *Nace Corrosion*; NACE: Bethlehem, PA, USA, 2012; p. NACE-2012-1559.
86. Liu, R.; Li, J.; Liu, Z.; Du, C.; Dong, C.; Li, X. Effect of pH and H_2S concentration on sulfide stress corrosion cracking (SSCC) of API 2205 duplex stainless steel. *Int. J. Mater. Res.* **2015**, *106*, 608–613. [CrossRef]
87. Tang, J.; Shao, Y.; Guo, J.; Zhang, T.; Meng, G.; Wang, F. The effect of H_2S concentration on the corrosion behavior of carbon steel at 90 °C. *Corros. Sci.* **2010**, *52*, 2050–2058. [CrossRef]
88. Taheri, H.; Kakooei, S.; Ismail, M.C.; Dolati, A. The effect of H_2S concentration and temperature on corrosion behavior of pipeline steel A516-Gr70. *Casp. J. Appl. Sci.* **2012**, *1*, 41–47.
89. Qi, Y.; Luo, H.; Zheng, S.; Chen, C.; Lv, Z.; Xiong, M. Effect of H_2S partial pressure on the tensile properties of A350LF2 steel in the absence and presence of pre-immersion. *Mater. Sci. Eng. A* **2014**, *609*, 161–167. [CrossRef]
90. Musayeva, N.; Khalilova, H.; Izzatov, B.; Trevisi, G.; Ahmadova, S.; Alizada, M. Highly selective detection of hydrogen sulfide by simple Cu-CNTs nanocomposites. *C* **2023**, *9*, 25. [CrossRef]
91. Khalid, H.U.; Ismail, M.C.; Nosbi, N. Permeation damage of polymer liner in oil and gas pipelines: A review. *Polymers* **2020**, *12*, 2307. [CrossRef]
92. Ali, M.A.H.; Baggash, M.; Rustamov, J.; Abdulghafor, R.; Abdo, N.A.-D.N.; Abdo, M.H.G.; Mohammed, T.S.; Hasan, A.A.; Abdo, A.N.; Turaev, S.; et al. An automatic visual inspection of oil tanks exterior surface using unmanned aerial vehicle with image processing and cascading fuzzy logic algorithms. *Drones* **2023**, *7*, 133. [CrossRef]
93. Cheng, L.; Lou, F.; Guo, W. Corrosion protection of the potassium silicate conversion coating. *Vacuum* **2020**, *176*, 109325. [CrossRef]
94. Al-Moubaraki, A.H.; Obot, I.B. Corrosion challenges in petroleum refinery operations: Sources, mechanisms, mitigation, and future outlook. *J. Saudi Chem. Soc.* **2021**, *25*, 101370. [CrossRef]
95. Groysman, A. Corrosion problems and solutions in oil, gas, refining and petrochemical industry. *KOM Corros. Mater. Prot. J.* **2017**, *61*, 100–117. [CrossRef]
96. Popoola, L.T.; Grema, A.S.; Latinwo, G.K.; Gutti, B.; Balogun, A.S. Corrosion problems during oil and gas production and its mitigation. *Int. J. Ind. Chem.* **2013**, *4*, 35. [CrossRef]
97. Umoren, S.A.; Solomon, M.M.; Saji, V.S. Corrosion inhibitors for sour oilfield environment (H_2S corrosion). In *Corrosion Inhibitors in the Oil and Gas Industry*; Wiley: Hoboken, NJ, USA, 2020; pp. 229–254.
98. Zhao, X.; Huang, W.; Li, G.; Feng, Y.; Zhang, J. Effect of CO_2/H_2S and applied stress on corrosion behavior of 15Cr tubing in oil field environment. *Metals* **2020**, *10*, 409. [CrossRef]
99. Dong, C.; Luo, H.; Xiao, K.; Sun, T.; Liu, Q.; Li, X. Effect of temperature and Cl^- concentration on pitting of 2205 duplex stainless steel. *J. Wuhan Univ. Technol. Mater. Sci. Ed.* **2011**, *26*, 641–647. [CrossRef]
100. Liu, H.; Hua, Y.; Shi, S.; Lin, X.; Neville, A.; Wang, Y.; Sun, J. Stability of passive film and pitting susceptibility of 2205 duplex stainless steel in CO_2/H_2S-containing geothermal environment. *Corros. Sci.* **2023**, *210*, 110832. [CrossRef]
101. Zheng, S.Q.; Chen, C.F.; Chen, L.Q. Corrosion characteristics of 2205 duplex stainless steel in high temperature and high pressure environment containing H_2S/CO_2. *Appl. Mech. Mater.* **2012**, *236*, 95–98. [CrossRef]

102. Thorhallsson, A.I.; Karlsdottir, S.N. Corrosion Behaviour of Titanium Alloy and Carbon Steel in a High-Temperature, Single and Mixed-Phase, Simulated Geothermal Environment Containing H_2S, CO_2 and HCl. *Corros. Mater. Degrad.* **2021**, *2*, 190–209. [CrossRef]
103. Karlsdottir, S.N.; Ragnarsdottir, K.R.; Thorbjornsson, I.O.; Einarsson, A. Corrosion testing in superheated geothermal steam in Iceland. *Geothermics* **2015**, *53*, 281–290. [CrossRef]
104. Kang, Y.; Leng, X.; Zhao, L.; Bai, B.; Wang, X.; Chen, H. Review on the corrosion behaviour of nickel-based alloys in supercritical carbon dioxide under high temperature and pressure. *Crystals* **2023**, *13*, 725. [CrossRef]
105. Silva, C.C.; de Miranda, H.C.; Motta, M.F.; Farias, J.P.; Afonso, C.R.M.; Ramirez, A.J. New insight on the solidification path of an alloy 625 weld overlay. *J. Mater. Res. Technol.* **2013**, *2*, 228–237. [CrossRef]
106. Guo, Q.; Li, Y.; Qian, J.; Yu, H.; Chen, C. Study of the pitting corrosion at welding joints of Inconel 625 alloy under high temperature and high H_2S/CO_2 partial pressure. *Int. J. Electrochem. Sci.* **2017**, *12*, 8929–8943. [CrossRef]
107. Montemor, M.F.; Simões, A.m.p.; Ferreira, M.G.S.; Belo, M.D.C. The role of Mo in the chemical composition and semiconductive behaviour of oxide films formed on stainless steels. *Corros. Sci.* **1999**, *41*, 17–34. [CrossRef]
108. Tomio, A.; Sagara, M.; Doi, T.; Amaya, H.; Otsuka, N.; Kudo, T. Role of alloyed molybdenum on corrosion resistance of austenitic Ni–Cr–Mo–Fe alloys in H_2S–Cl^- environments. *Corros. Sci.* **2015**, *98*, 391–398. [CrossRef]
109. Gao, X.; Liu, M. Corrosion behavior of high-strength C71500 copper-nickel alloy in simulated seawater with high concentration of sulfide. *Materials* **2022**, *15*, 8513. [CrossRef]
110. Sun, S.; Wang, H.; Zhang, L.; Hao, Y.; Li, C.; Hu, S. Intergranular-stress corrosion cracking mechanism of brass in H_2S environment: A DFT study. *Comput. Mater. Sci.* **2019**, *170*, 109193. [CrossRef]
111. Li, H.; Zhang, X.; Chu, H.; Qi, G.; Ding, H.; Gao, X.; Meng, J. Molecular simulation on permeation behavior of $CH_4/CO_2/H_2S$ mixture gas in PVDF at service conditions. *Polymers* **2022**, *14*, 545. [CrossRef]
112. Maraveas, C. Durability issues and corrosion of structural materials and systems in farm environment. *Appl. Sci.* **2020**, *10*, 990. [CrossRef]
113. Hussain, M.; Zhang, T.; Chaudhry, M.; Jamil, I.; Kausar, S.; Hussain, I. Review of prediction of stress corrosion cracking in gas pipelines using machine learning. *Machines* **2024**, *12*, 42. [CrossRef]
114. Xie, M.; Tian, Z. A review on pipeline integrity management utilizing in-line inspection data. *Eng. Fail. Anal.* **2018**, *92*, 222–239. [CrossRef]
115. Vakili, M.; Koutník, P.; Kohout, J. Corrosion by Polythionic Acid in the Oil and Gas Sector: A Brief Overview. *Materials* **2023**, *16*, 7043. [CrossRef]

Disclaimer/Publisher's Note: The statements, opinions and data contained in all publications are solely those of the individual author(s) and contributor(s) and not of MDPI and/or the editor(s). MDPI and/or the editor(s) disclaim responsibility for any injury to people or property resulting from any ideas, methods, instructions or products referred to in the content.